

Pictorial essay:

All rights reserved © K H Fung / Tridactyls.org

VIRTUAL AUTOPSY OF NAZCA TRIDACTYL MUMMY ‘MARIA’

A scientific study using CT scan with advanced 3D image reconstruction and virtual dissection.

By **Dr. K.H. Fung** (Hong Kong SAR, China)

(latest update 30 Dec 2025)

ACKNOWLEDGEMENT

- The author wished to thank Tridactyls.org for granting permission for use of the DICOM CT datasets available on their website for this scientific study.

SECTION I: PRESERVATION STATUS OF ‘MARIA’

- ‘Maria’ (*Figure 1*) was found to be a very well preserved, desiccated and complete corpse discovered in the Peruvian desert in Nazca in 2017 (strictly speaking not a mummy as commonly mentioned).
- It was found in a foetal position with head and neck tilted towards the right side. (*Figures 2,3*) Contracted and detached bi-lobed brain remnant was found located in the posterior aspect of the cranium suggesting that it had been in a right lateral decubitus position after death. Additional separated smaller brain remnants were found in left middle cranial fossa and in posterior fossa bilaterally. (*Figure 4*)
- Skin, bones, ligaments and tendons were well preserved. (*Figures 2,3,5,6,7*)
- Although soft tissue organs had been replaced by air, their covering connective tissue and fascia remained. The heart (*Figure 8*) can be identified and retained its normal configuration. Great vessels, lungs, tracheo-bronchial tree can also be identified.
- ‘Maria’ had broken, poorly aligned and irregular sets of teeth (*Figure 9*). The upper incisors were particularly affected suggesting that Maria may be using the mouth to bite hard object habitually. Dental caries were noted.
- Structures resembling lens suggestive of cataract could be located in both orbits. (*Figure 10*) The large partially collapsed eyeballs were identifiable. (*Figure 34*)
- Coprolites were noted in bowel. (*Figure 11*) Seed could be identified within coprolite suggestive of vegetarian-based diet.
- Gross degenerative changes in spine provided documentary evidence of an erect bipedal posture showing aging change. (*Figure 12*)

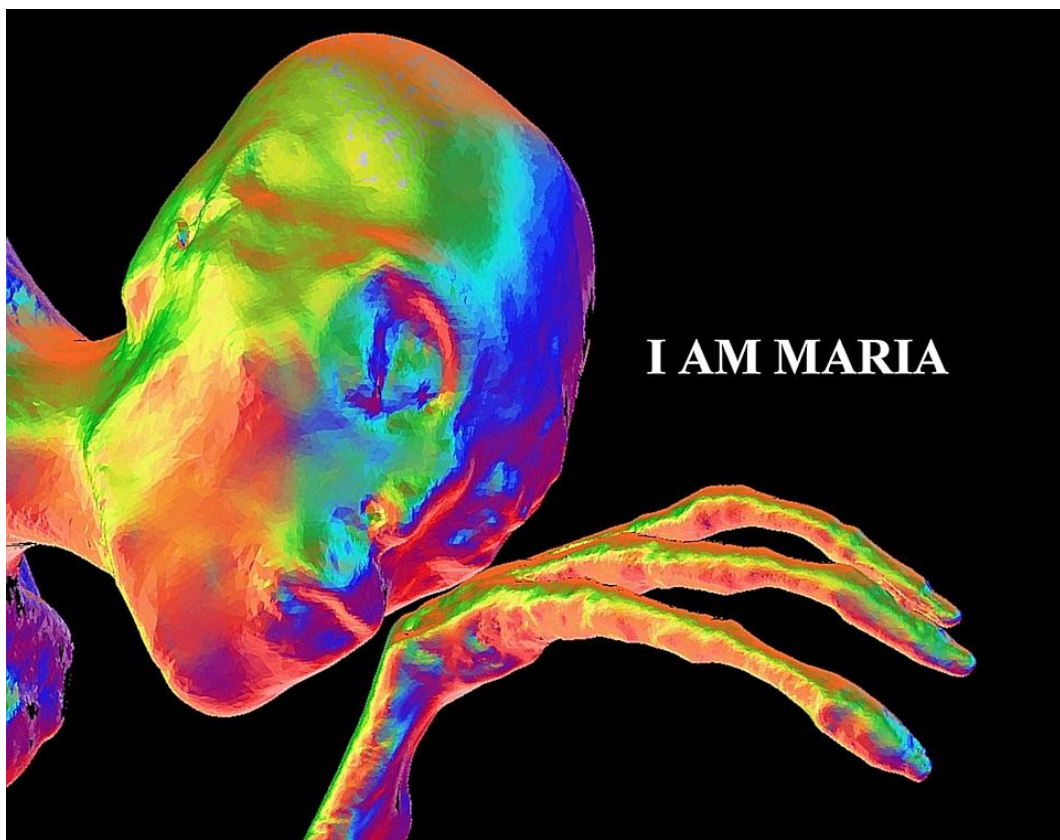


Figure 1: Artwork created from 3D CT showing the face of 'Maria' and her tridactyl hand with very long fingers.

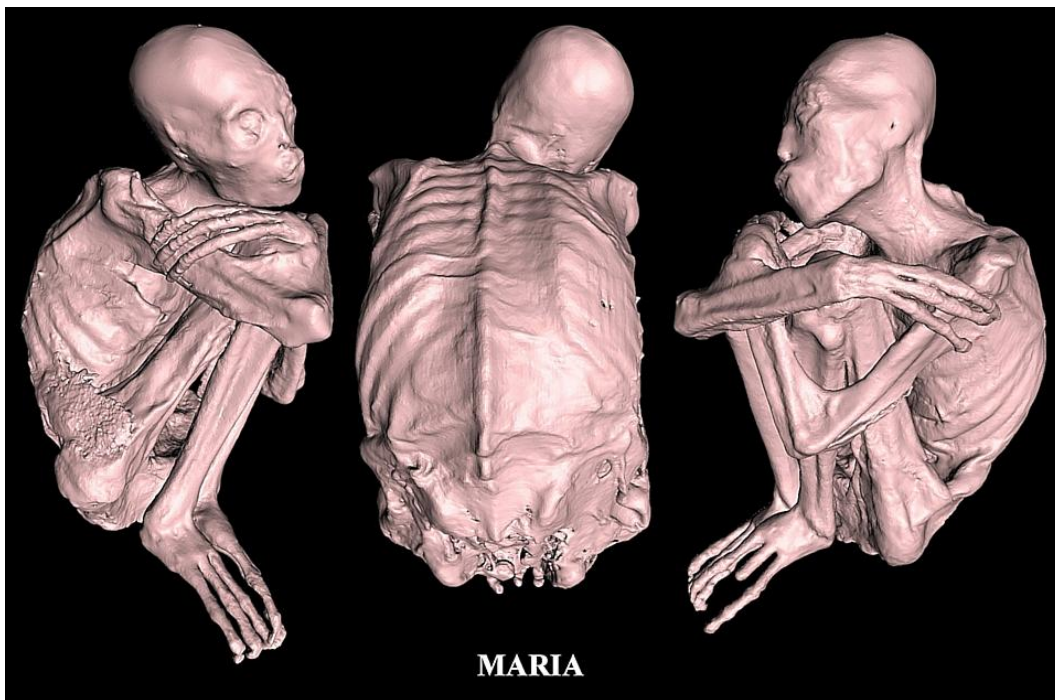


Figure 2: 3D CT of 'Maria' showing posture in foetal position with head tilted towards the right side, upper limb wrapping around the knees thence obscuring the front of the chest and abdomen. Note the very long multi-segmented fingers in tridactyl hands and feet.

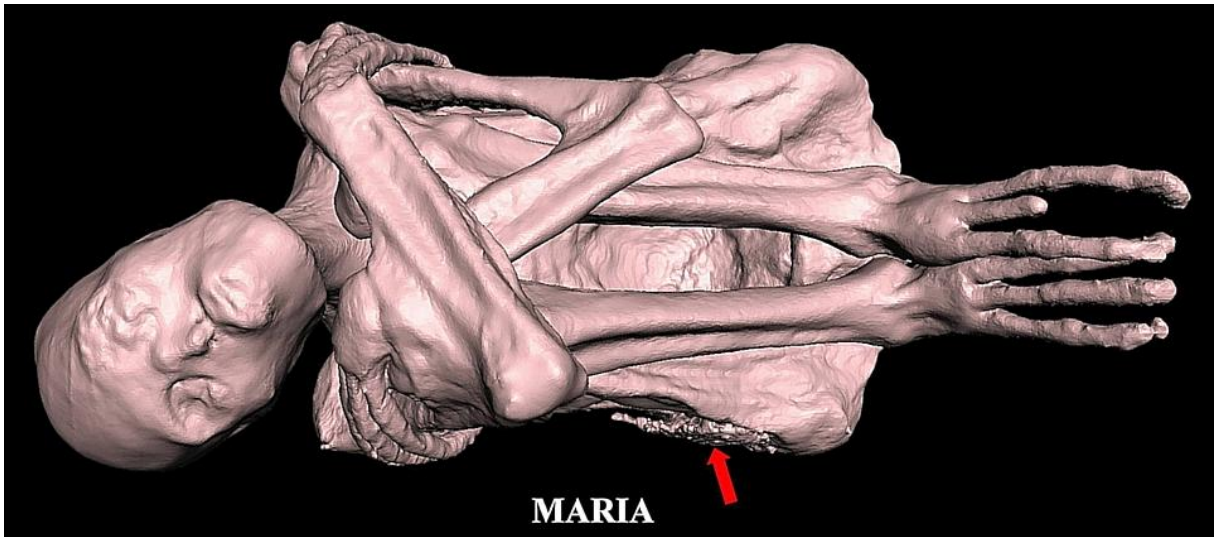


Figure 3: 3D CT showing 'Maria' lying on right side. A layer of extraneous material was found in her right iliac region (*red arrow*).

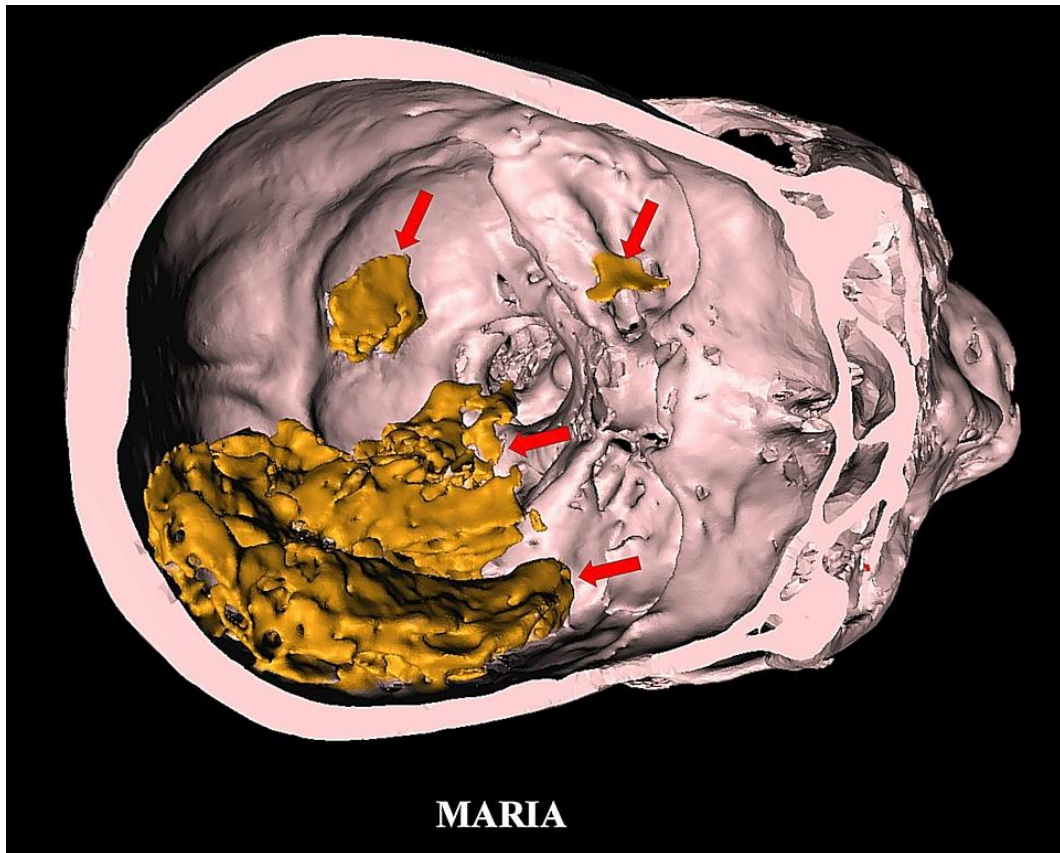


Figure 4: 3D CT showing cut section of cranium. Note the bi-lobed brain remnant (*red arrows*) in dependent position on right side with smaller pieces of brain tissues scattered in middle and posterior cranial fossae.

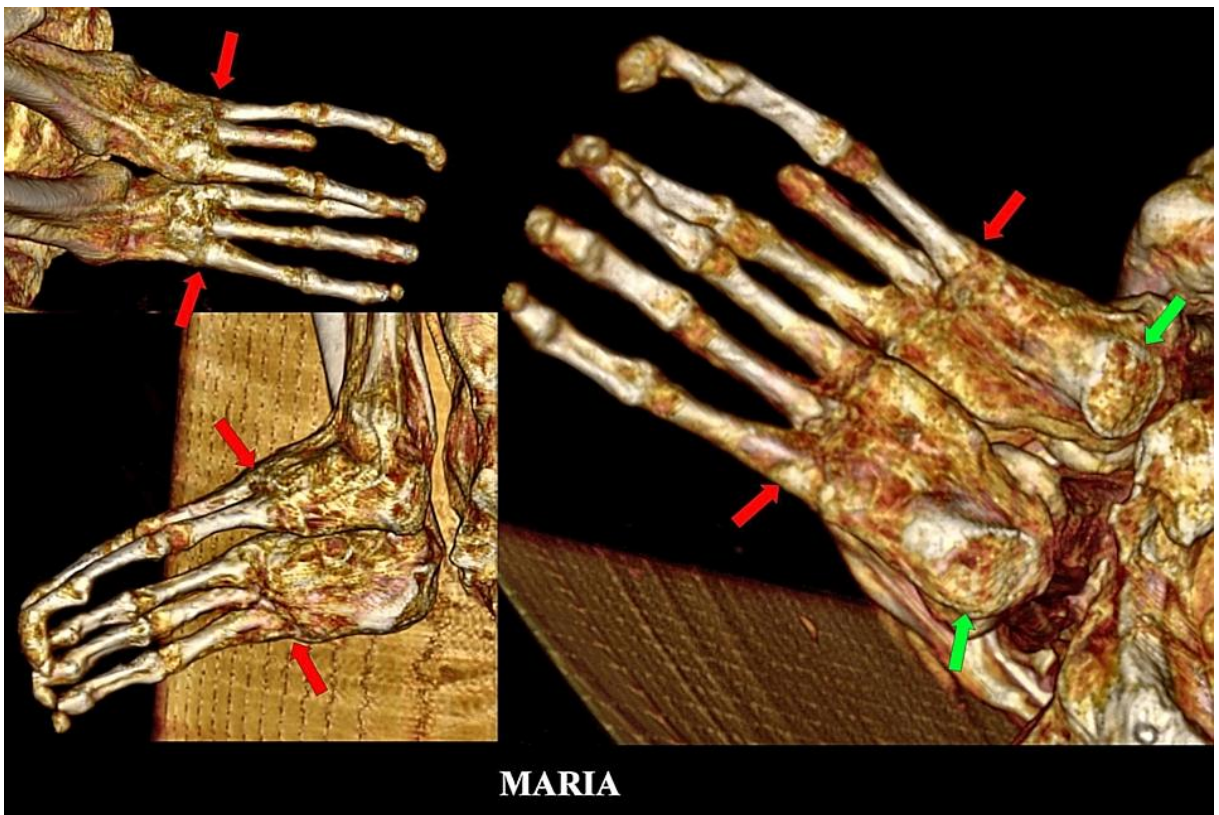


Figure 5: Volume rendered 3D CT of tridactyl feet. Note the well aligned intact joints between tarsal bones and digits (*red arrows*). A rather flat surface with thin cortex (*green arrows*) can be found in posterior parts of bilateral calcanei suspicious of truncation of the bones.

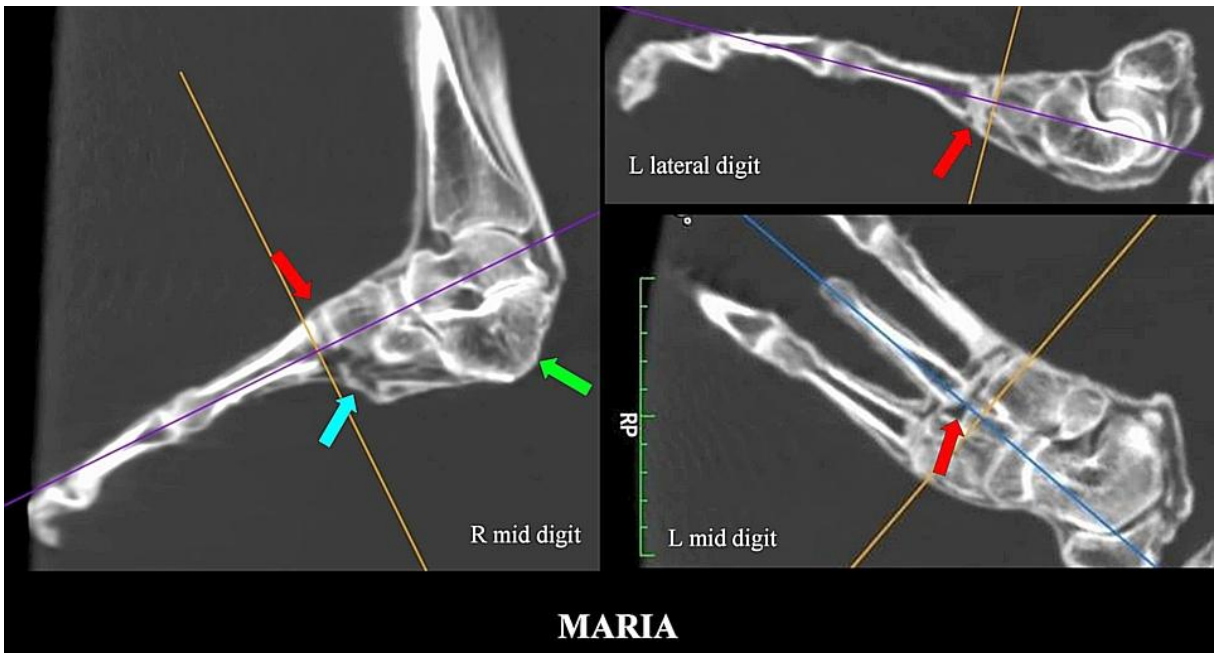


Figure 6: Oblique plane multi-planar 2D CT reconstruction along digits showing the intact joints between digits and tarsal bones (*red arrows*). Note the shortening of the calcaneum with thinning of cortex posteriorly (*green arrow*) suspicious of previous bone truncation. Note the transition of thick soft tissue on the under-surface of the foot to the thin soft tissue of the digit (*blue arrow*).

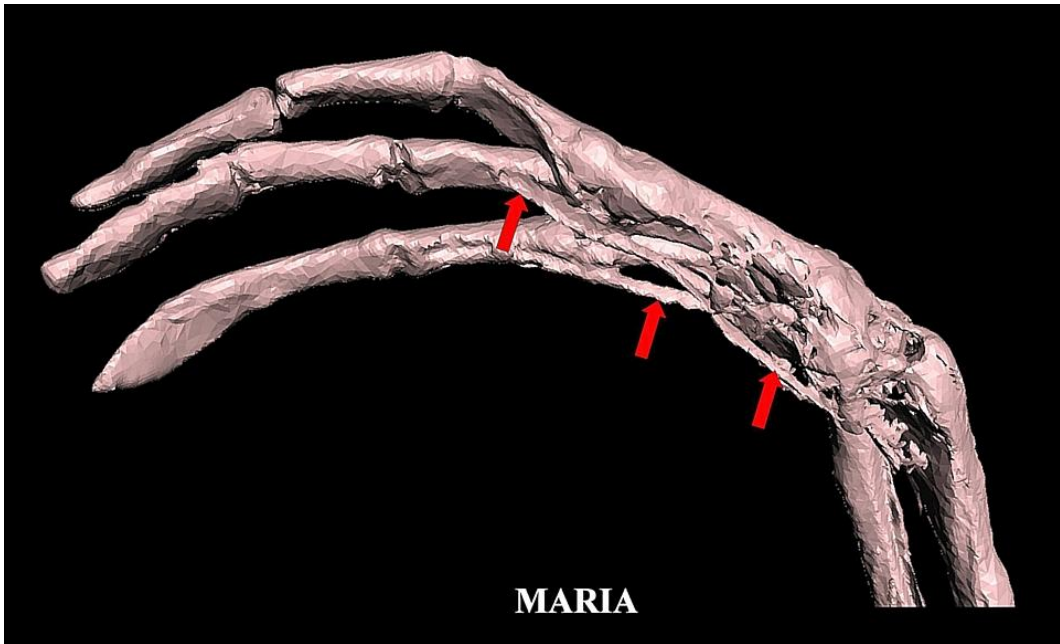


Figure 7: 3D CT of right hand showing intact tendons and ligaments (*red arrows*).

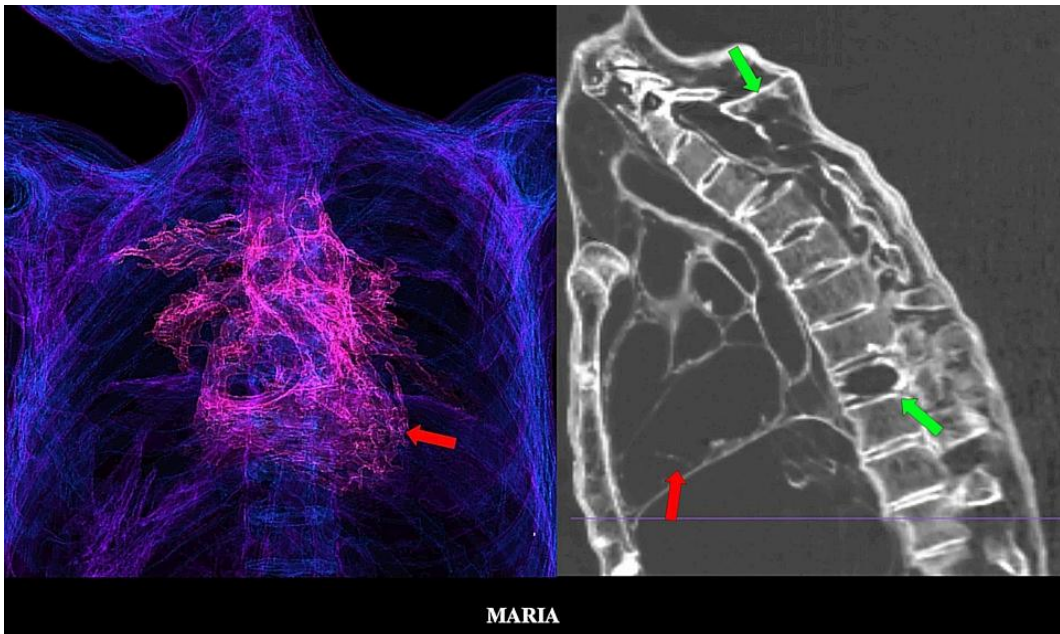


Figure 8: 3D CT showing the scaffolding of the heart (*red arrows*) showing normal shape. Destructive bone lesions can be identified in spine (*green arrows*).

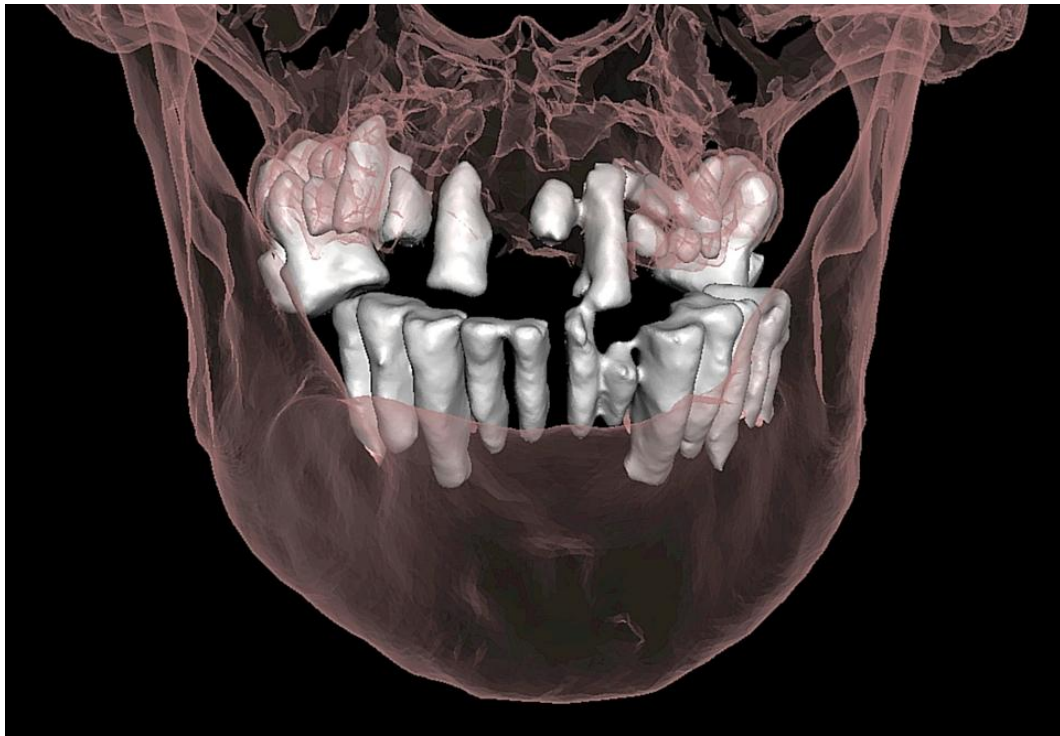


Figure 9: 3D CT showing the set of irregular teeth with broken teeth in upper set anteriorly.

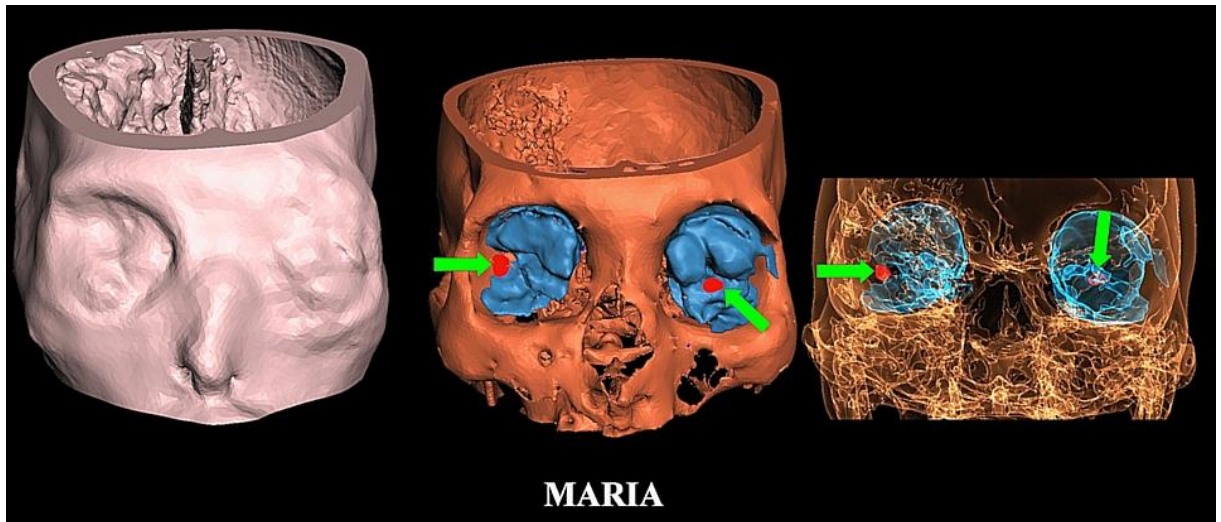


Figure 10: 3D CT. Bone and ocular contents (*in blue*) are seen (*middle*) with semi-transparent view (*right*). *Green arrows* point to suspected lens structures (*in red*). Swellings were noted in left upper and lower eyelids and in adjacent left forehead as shown in surface view (*left*).

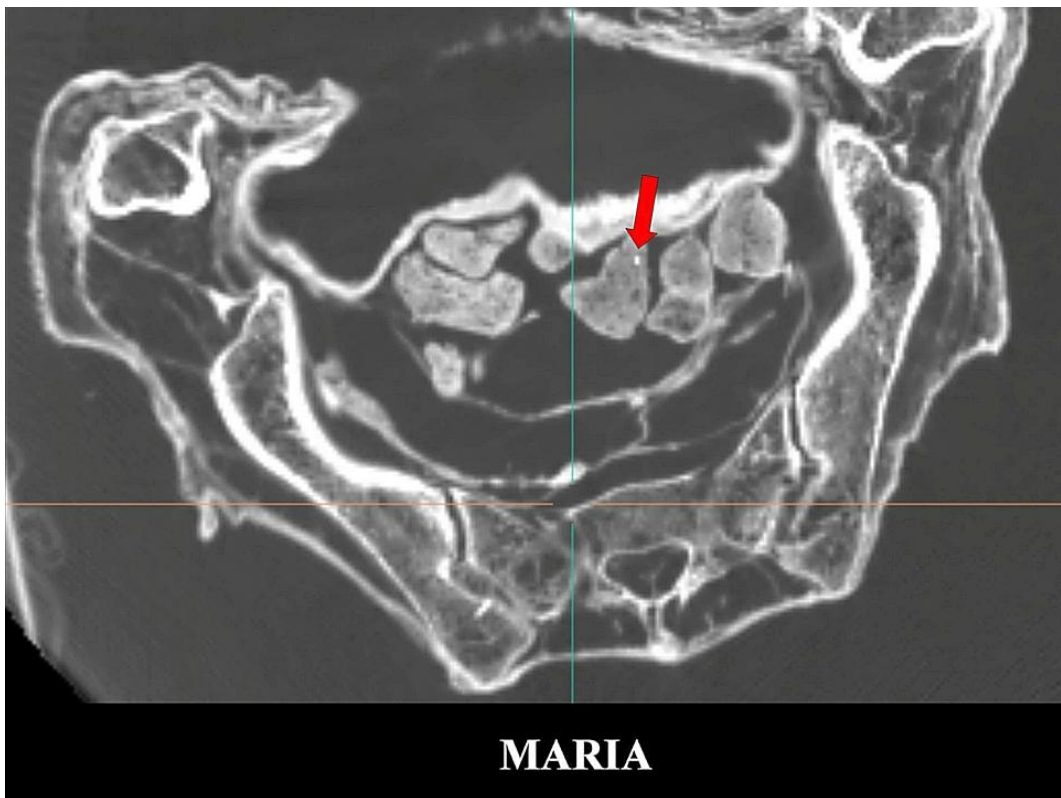


Figure 11: 2D CT axial scans showing multiple coprolites in abdomen and pelvis, one of them containing a seed (*red arrow*) suggestive of vegetative diet.

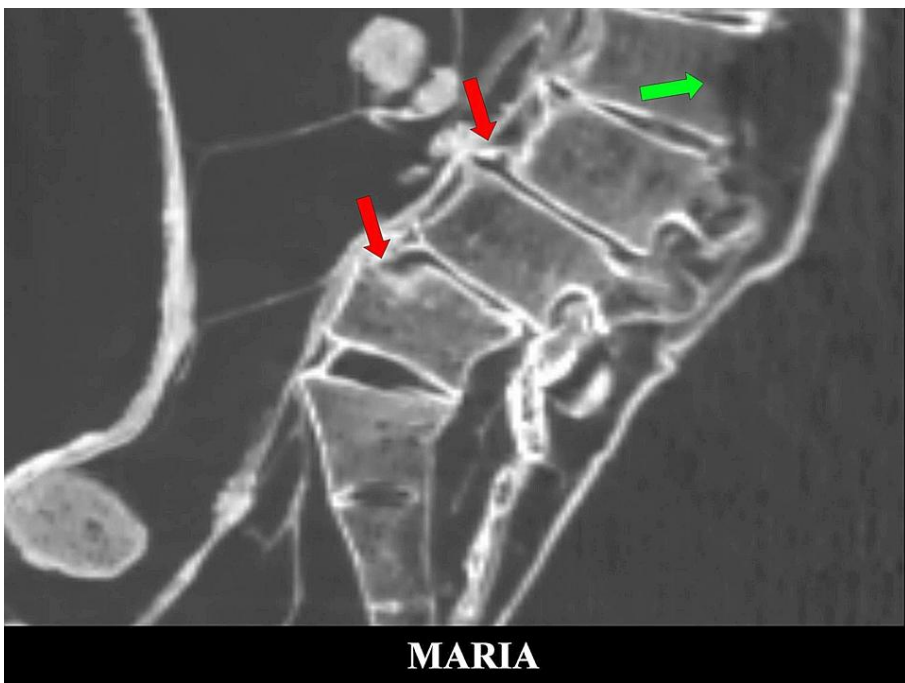


Figure 12: 2D CT sagittal scan showing degenerative changes in lumbar spine with retro-spondylolisthesis (*red arrows*) in L3/4 and L4/5, narrowing of intervertebral spaces and spondyloarthropathies. Osteolytic lesion (*green arrow*) in posterior elements of L2 lumbar spine suggestive of cancer with bony secondary.

SECTION II: EVIDENCES OF ANATOMICAL ANOMALIES IN 'MARIA'

- 'Maria' has abnormal craniofacial features (*Figure 13*) with mildly elongated skull with shifting of vertex posteriorly, sloping face and forehead (*Figure 14*), widely separated sloping enlarged orbits, small nose deviated towards the right with small bilateral nostrils, protruding upper and lower jaws, prominent mandible, absence of pinnae and presence of external auditory canal openings.
- The cranium showed shallow anterior cranial fossa, thickened skull bones posteriorly and absence of identifiable coronal or sagittal sutures on its outer or inner surfaces (*Figures 14, 15*). The inner surface of the skull bone was rather smooth. Lambdoid suture was present although not conspicuous and without Wormian bones.
- 3D digital endocast confirmed small frontal lobes (*Figure 16*). Computerized direct volume measurement of endocast yielded a volume of 1195356 mm³. (*Figure 36*)
- Tridactyls with exceptionally long fingers and toes (*Figures 17.18.19*) were hallmark features. 5 segments were noted in each digit in hands and 4 segments in each digit in feet.
- Mildly depressed lower sternum (pectus excavatum) was noted. (*Figure 20*)
- Umbilicus (navel) cannot be found. (*Figure 20*)
- Broad anterior pubic region with presence of a small midline 'phallus-like' structure could be found. (*Figure 20*)

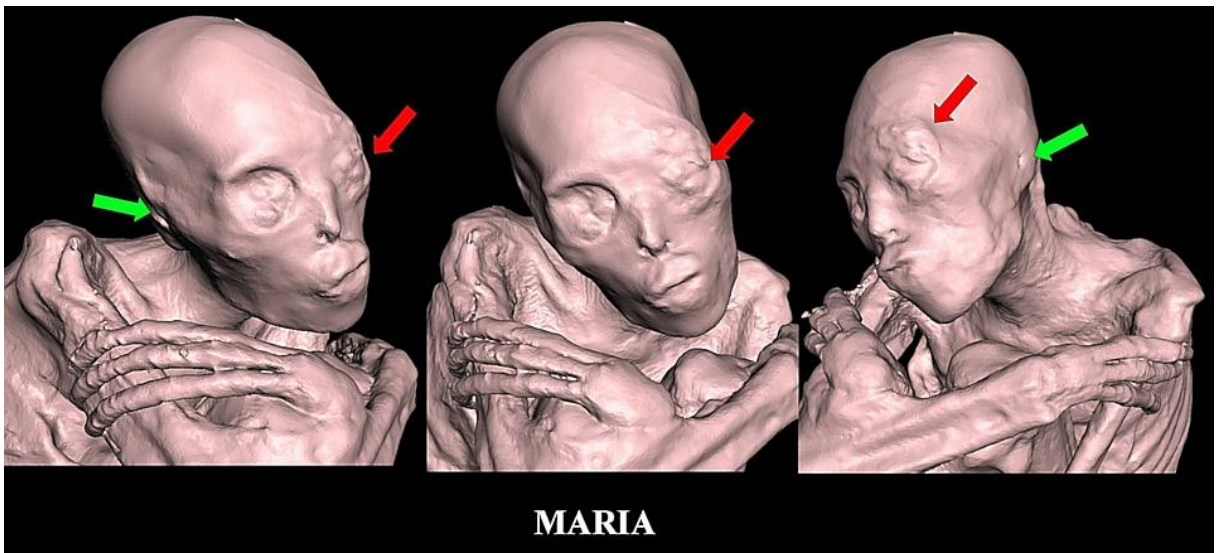


Figure 13: 3D CT showing anomalous facial features. 'Maria' has a slightly narrowed and elongated skull, shallow forehead, sloping and elongated face, bilateral large rounded eye sockets, small nose deviated towards the right side with 2 small nostrils, prominent protruding upper and lower jaws showing prominent lips. Irregular soft tissue swelling was noted in left eye socket extending to left forehead (*red arrows*). No external pinnae bilaterally. Small ear openings (*green arrows*) communicating with external auditory meati.

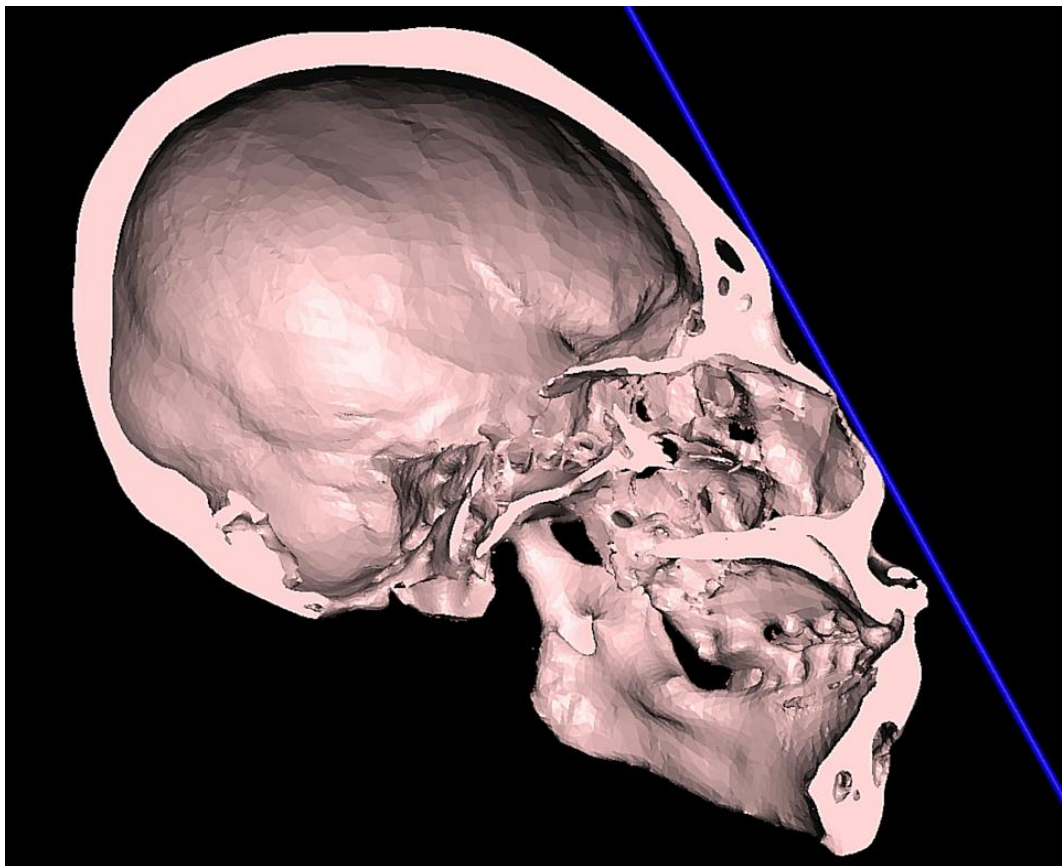


Figure 14: Sagittal section of skull showing the sloping face and frontal skull with anterior shift of the maxillary bone and mandible. The anterior cranial fossa was small. Thickening of skull vault with lack of identifiable coronal suture on its inner surface. Pituitary fossa was not enlarged.

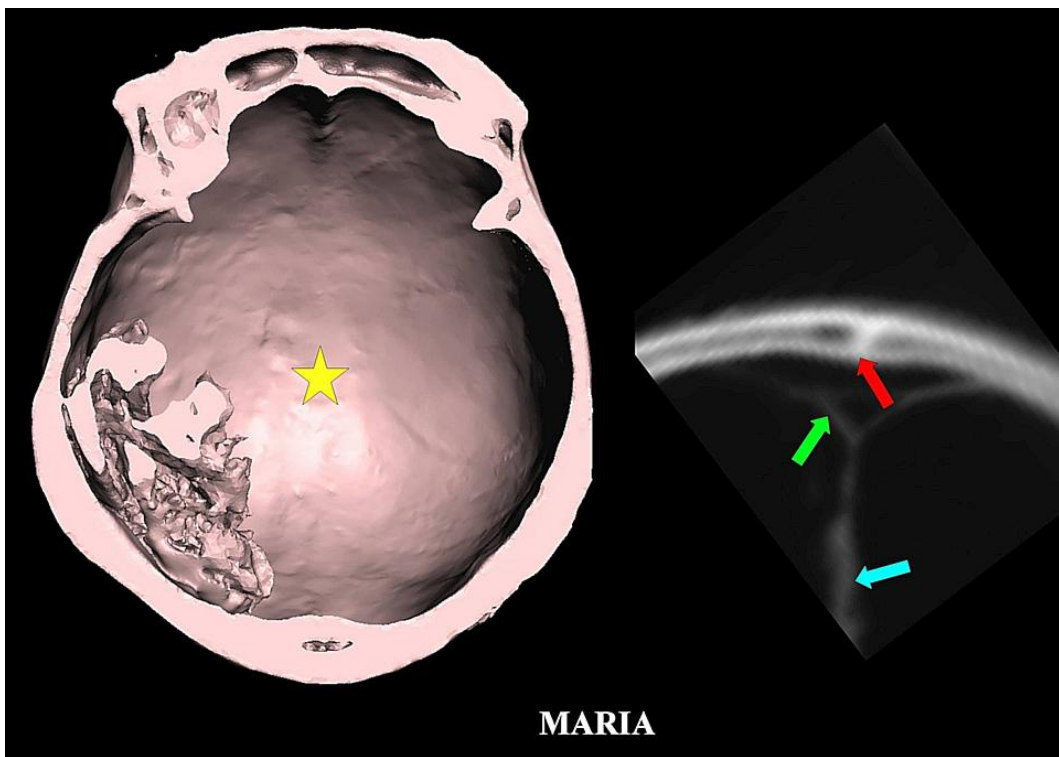


Figure 15: 3D CT inferior view of cut section of skull vault (*left*) showing smooth inner surface with lack of identifiable sagittal suture (location of *yellow star*) and coronal suture. Skull bone appeared thick posteriorly. Brain remnant was noted on right side. 2D coronal CT scan (*right*) showing the fused suture (*red arrow*) within bone with continuous inner and outer tables. Superior sagittal sinus (*green arrow*) and falx cerebri (*blue arrow*) were also noted.

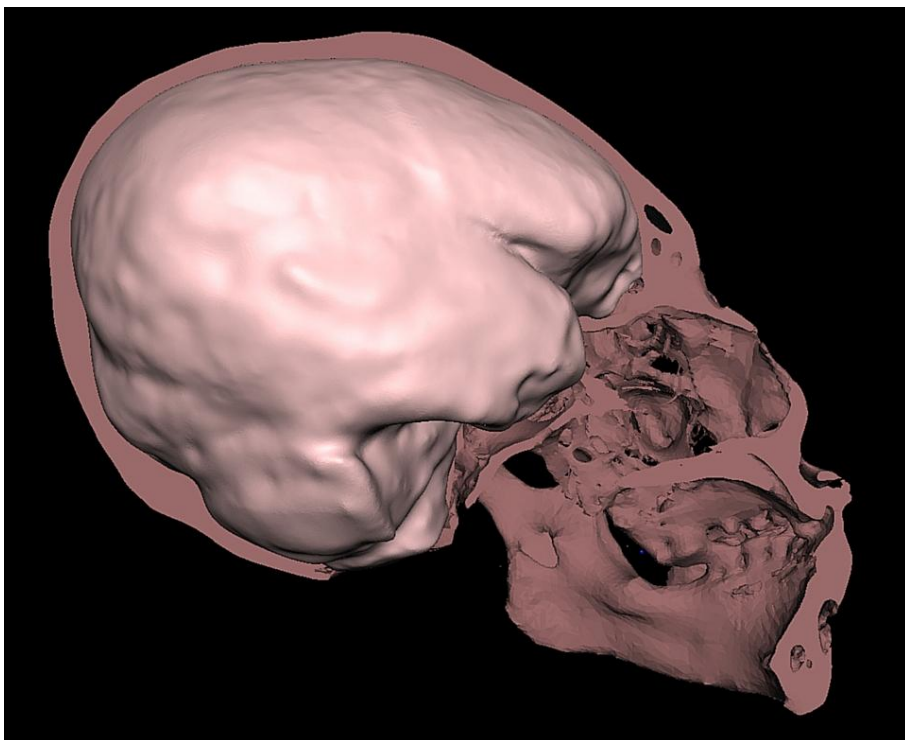


Figure 16: 3D CT digital cranial endocast showing relatively small frontal lobes fitted into sagittal section of skull.



Figure 17: 3D CT showing both hands, each with 3 digits resting on both arms. Note the flexibility of the slender long fingers.

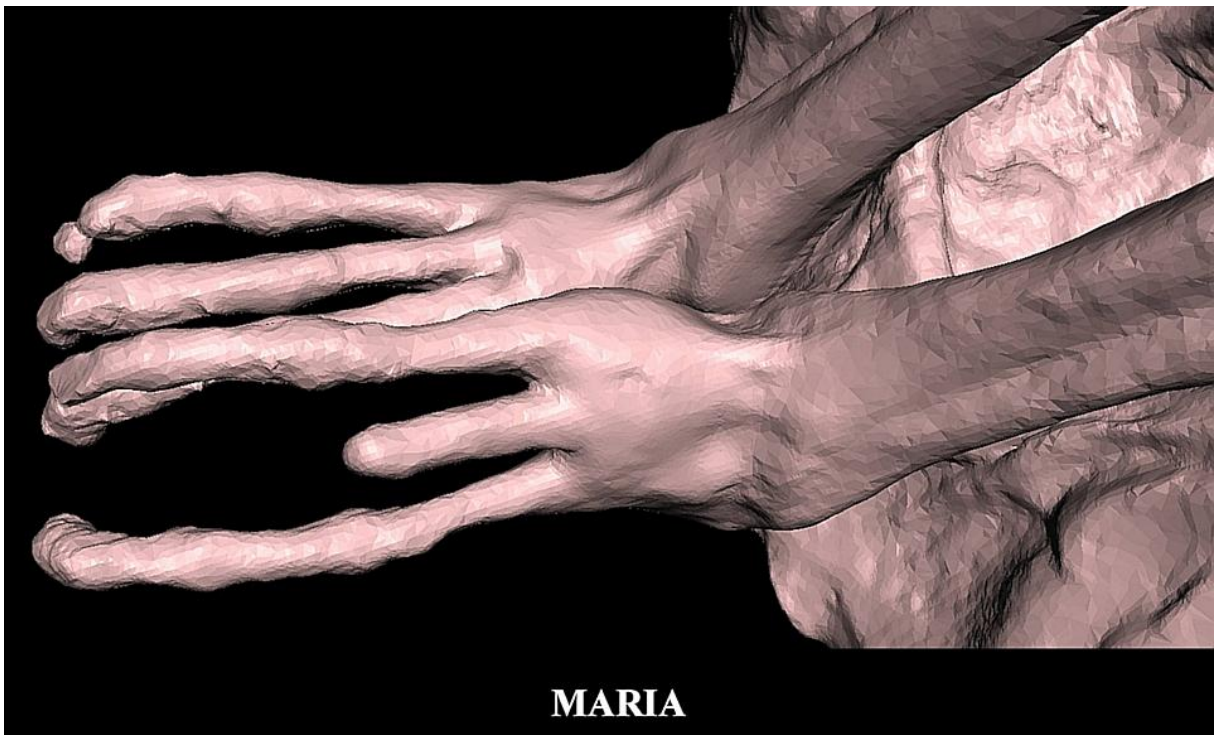


Figure 18: 3D CT showing tridactyl feet showing claw like deformity at the ends of digits.

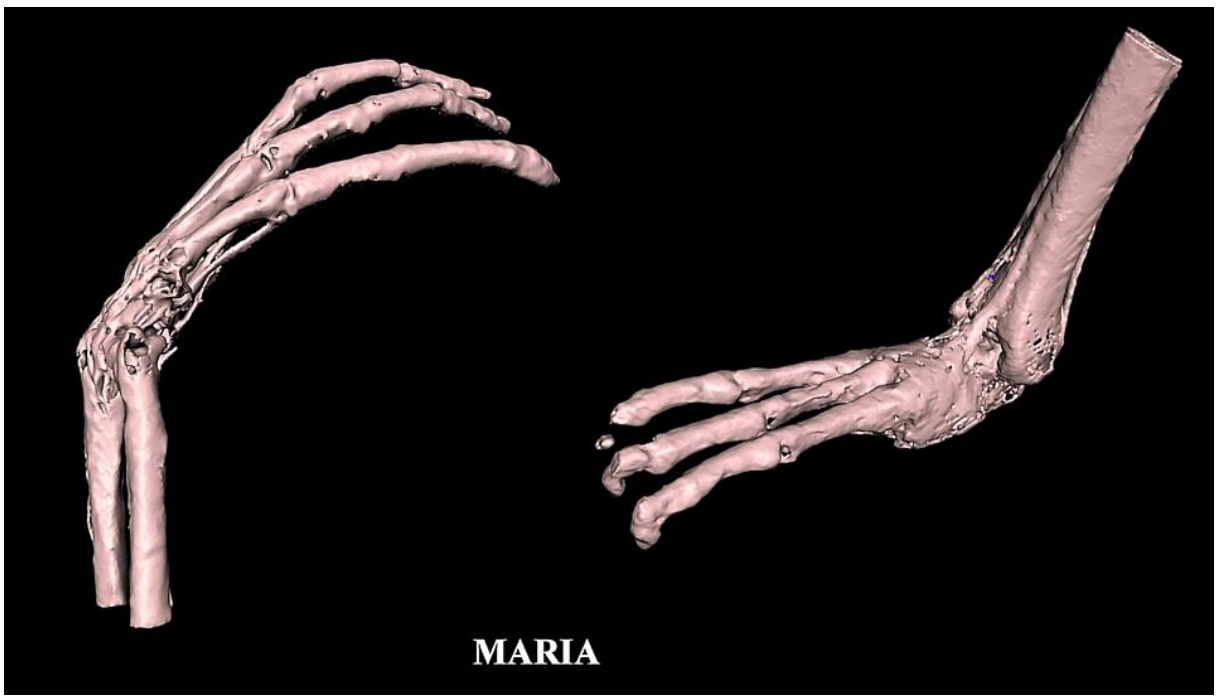


Figure 19: 3D CT of right hand (*left*) and right foot (*right*). Note presence of 5 segments in each finger and 4 segments in each toe.

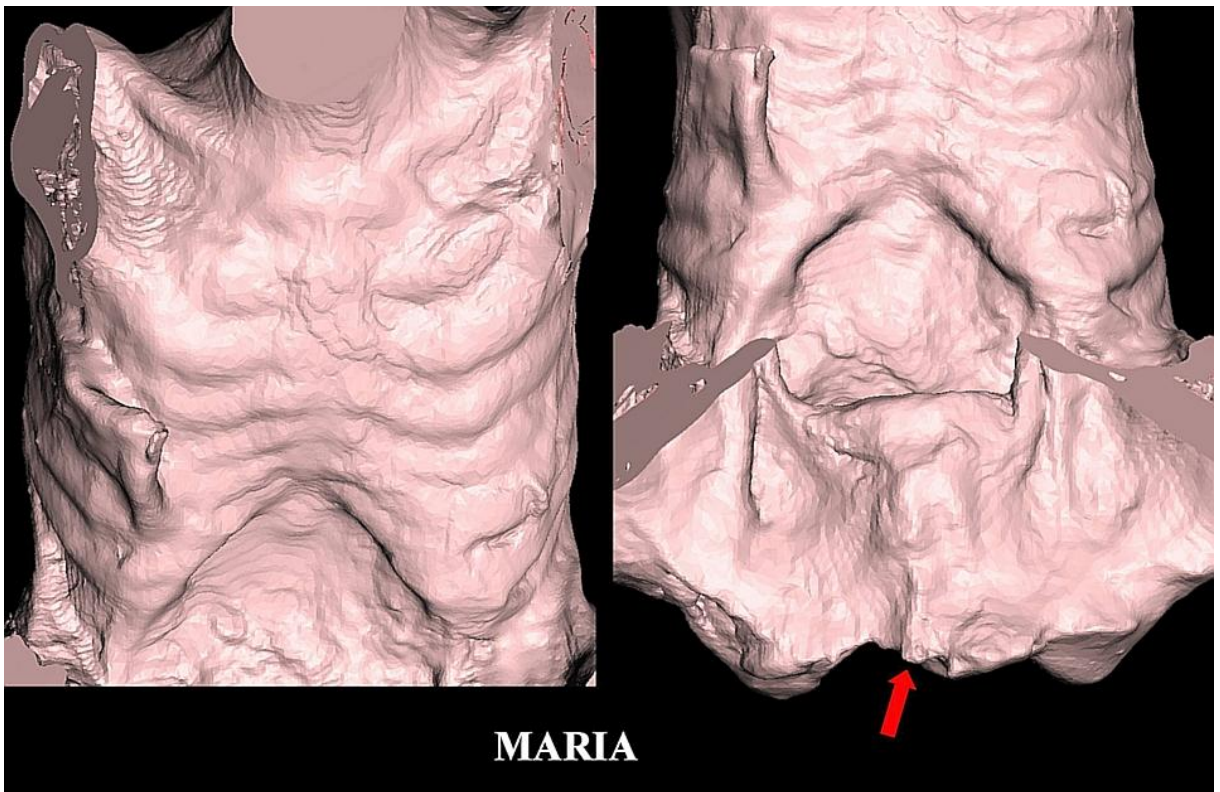


Figure 20: 3D CT showing depressed lower sternum in anterior chest wall (*left*) and broad flat pubic region with small midline pointed structure suggestive of phallus / clitoris (*red arrow*).

SECTION III: EVIDENCES OF DISEASES IN ‘MARIA’

- Multiple osteolytic bone lesions suggestive of extensive bony secondaries from disseminated cancer can be found in spine at T2-4, T8 and T12-L2 levels (*Figure 21*) and in acetabula of both hips. (*Figure 22*). The lesions in posterior elements of T2-4 caused anterior spondylolisthesis of T3 on T4. Associated partial collapse of T8 and L1 vertebral bodies were present.
- Flattened and well-formed right breast with nipple can be located in right antero-lateral thorax but cannot be found on left side. Instead linear raised structures were found at expected location of left breast raising suspicion of mastectomy scar following surgical removal. (*Figure 23*)
- Few tiny calcified foci and fibrotic scarrings were found in both lungs. (*Figure 24*)

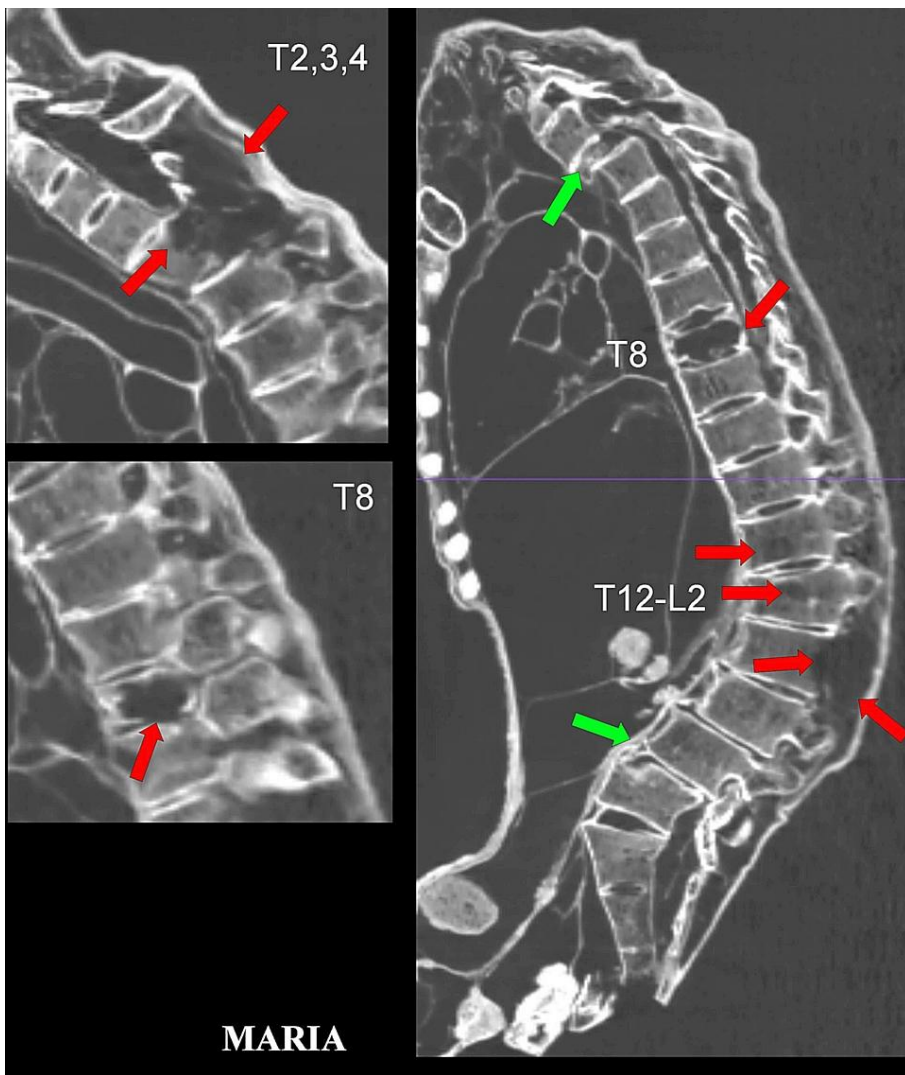


Figure 21: 2D sagittal CT scans showing multiple osteolytic bone lesions (*red arrows*) in thoracic and lumbar spine. Degenerative spinal changes causing retro-spondylolisthesis were noted in L3/4 and L4/5 (*green arrows*).

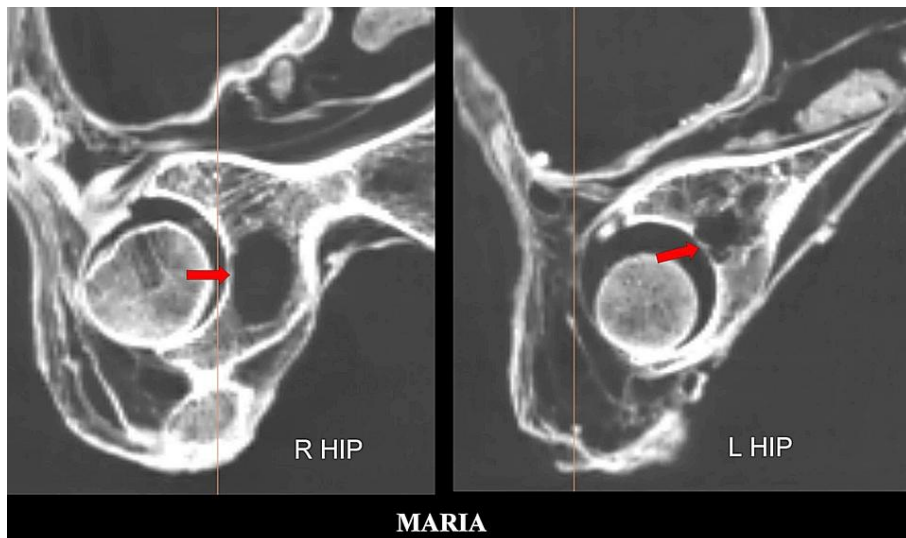


Figure 22: 2D sagittal CT scans showing osteolytic bone lesions (*red arrows*) in acetabula of both hips.

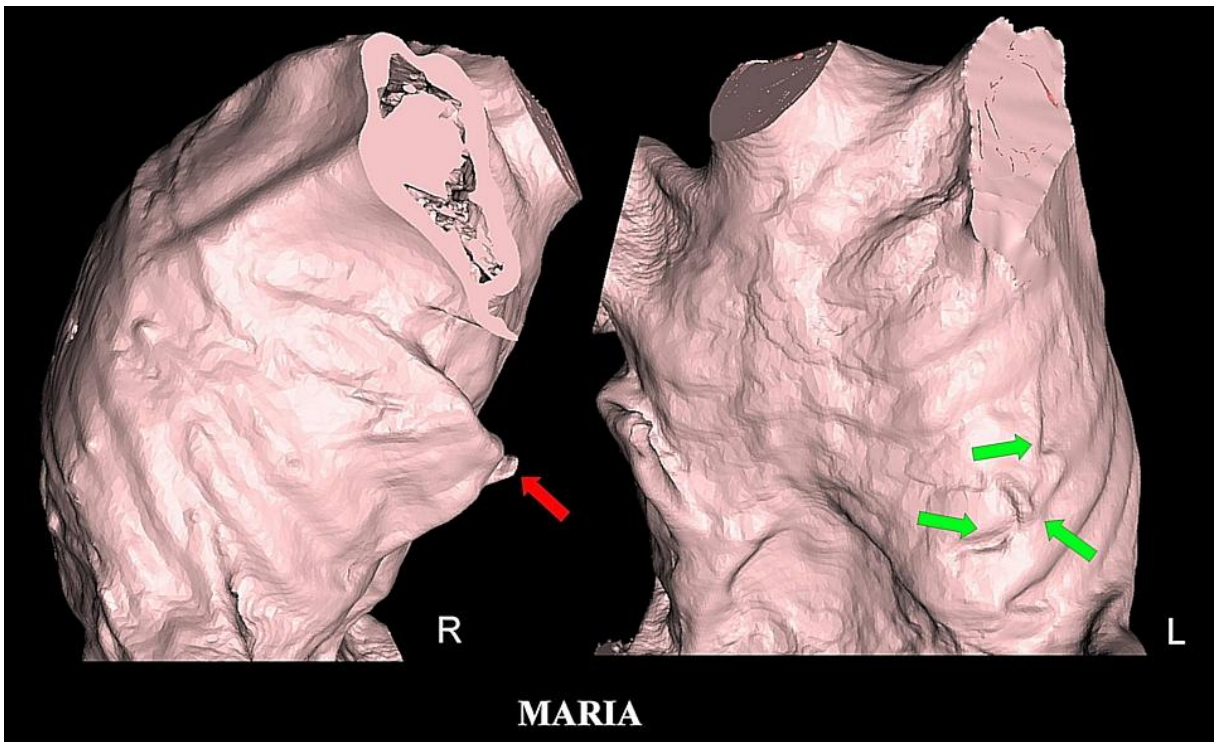


Figure 23: 3D CT showing flattened well developed right breast (*left image*) with nipple (*red arrow*). The left breast (*right image*) was not found and replaced by linear raised edges (*green arrows*) suggestive of surgical scars.

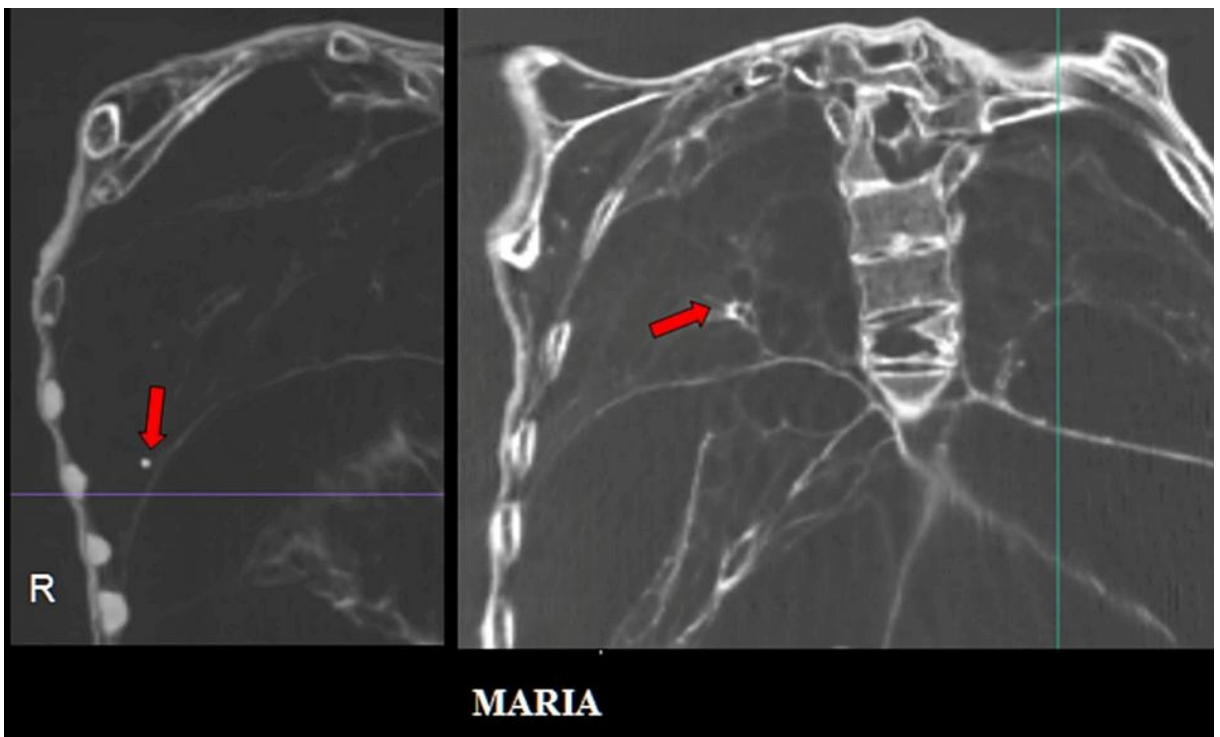


Figure 24: 2D sagittal (*left*) and coronal (*right*) CT scans showing tiny calcified foci (*red arrows*) and small fibrotic scarrings in both lungs.

SECTION IV: EVIDENCE OF TRAUMATIC INJURIES AND FOREIGN BODIES

- Large area of tissue loss (*Figures 25,27*) was found in the sacral and perineal areas. There was deep involvement with gaping underlying pelvic floor resulting in exposure of bowel loops containing coprolites. The sacrum was involved and transacted at S3 level. The broken distal fragment of sacrum was located slightly more anteriorly near the cut end (*Figure 26*). However no fracture was found in ischial tuberosities nor hips.
- Round shallow puncture holes (at least 7) were found scattered around the area of tissue loss. (*Figure 25*).
- At the left edge of the truncated sacrum, a bony cavity (*Figures 27,28*) was found extending superiorly into lower left sacro-iliac joint. The bony cavity contained a hexagonal shaped metallic foreign body with attached plate-like metallic component posteriorly. (*Figure 29*) The plate-like component showed rough anterior surface with smooth posterior surface. Smaller metallic particles were also found, including one at the entrance. The rest of the cavity was filled with mineral content such as grit.
- The posterior part of bilateral calcanei were truncated with evidence of regrowth of thin bony cortices. (*Figures 5,6,30, 31,38,39*) Adjacent attachment parts of bilateral Achilles tendons were cropped, more in left heel. (*Figures 30,31,38,39*)
- Both feet showed evidence of mutilations. (*Figure 32*) Of the 4 segments (S1-4 proximal to distal) in middle digit of left foot, only the proximal segment (S1) remained. The S3 and S4 segments of lateral digit of right foot were separated by partial amputation connected only by constricted skin. The dorsal parts of S3 and S4 segments of right middle digit and S4 segment of left medial digit appeared to have been sharply shaved off.
- Mutilation was also evident in the right hand. (*Figure 33*) Of the 5 segments (S1-5 proximal to distal) in medial digit, amputation of the most distal aspect of S3 segment was noted. There was partial subluxation of S3/4 joint. Asymmetrical subperiosteal bone formation causing bony thickening were noted on radial sides of S2 and S4 segments of medial digit.
- Focal calcifications or metallic foreign bodies were found inside the swollen left upper and lower eyelids (*Figure 34*)
- In the right buccal wall adjacent to right upper first and second molar teeth, an irregular structure was found suggestive of mineral content or foreign body, e.g. grit, containing multiple tiny focal calcifications (*Figure 35*). A tiny skin puncture hole was found overlying the lesion.

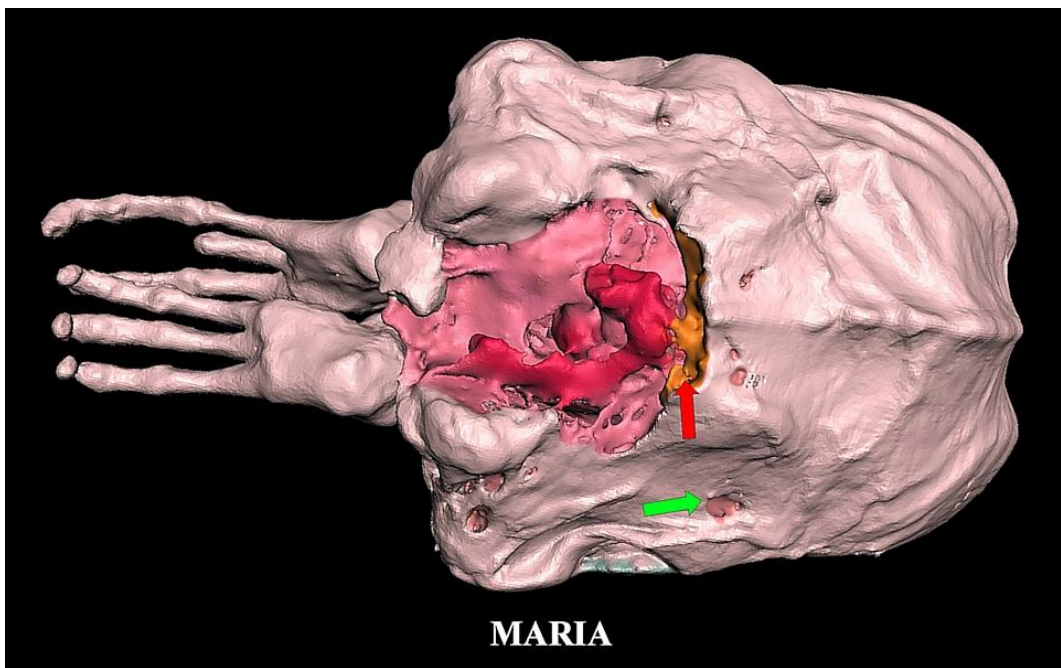


Figure 25: Large area of tissue loss (*in pink*) was present in the sacral area and perineum exposing underlying tissue plane with bulging bowel containing coprolites. The sacrum was transacted (*red arrow*). Multiple shallow puncture holes (*green arrow*) were found in surrounding area.

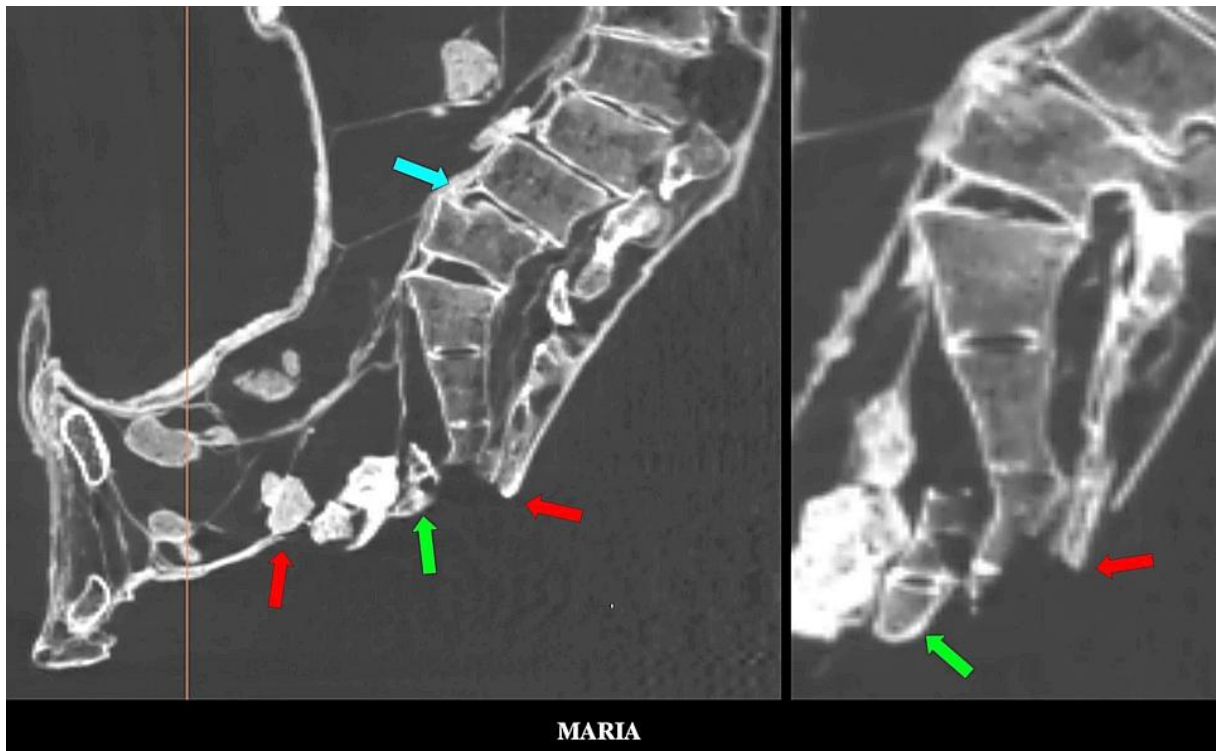


Figure 26: 2D sagittal CT scans showing extensive defect (*red arrows*) in sacral and perineal areas. (*left*) The sacrum (*right*) was transacted at S3 level with fracture fragment (*green arrow*) located slightly more anteriorly.

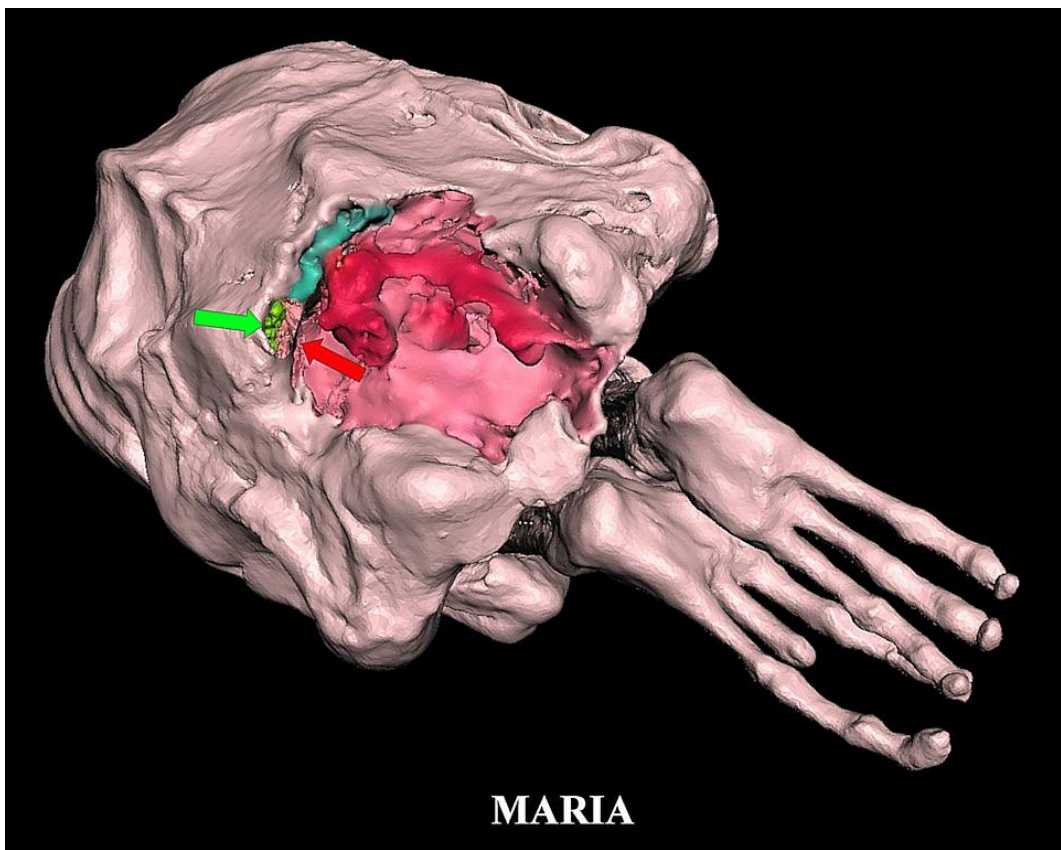


Figure 27: At the left margin of the transected sacrum, a pocket shaped hole (*red arrow*) was found extending superiorly into the left sacro-iliac joint. Inside the cavity, there was a shaped metallic foreign body (*green arrow*) and smaller metallic particles. The rest of the cavity was filled by grit.

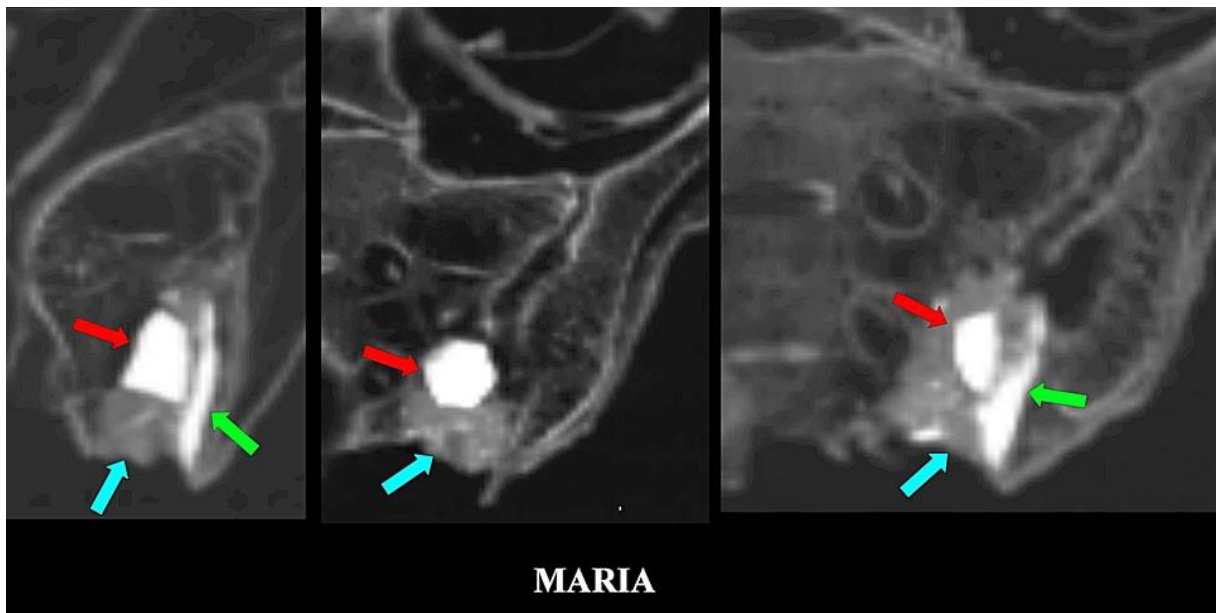


Figure 28: 2D sagittal (*left*) and coronal (*middle, right*) CT scans showing the entrance to the bony cavity (*blue arrows*) at truncated edge of the sacrum on the left side extending upwards toward left sacro-iliac joint. The cavity was filled with grit. A hexagonal shaped metallic foreign body (*red arrows*) with an attached plate-like metallic foreign body with rough anterior surface and smooth posterior surface (*green arrow*) was found inside the cavity. Smaller metallic fragment were also noted.

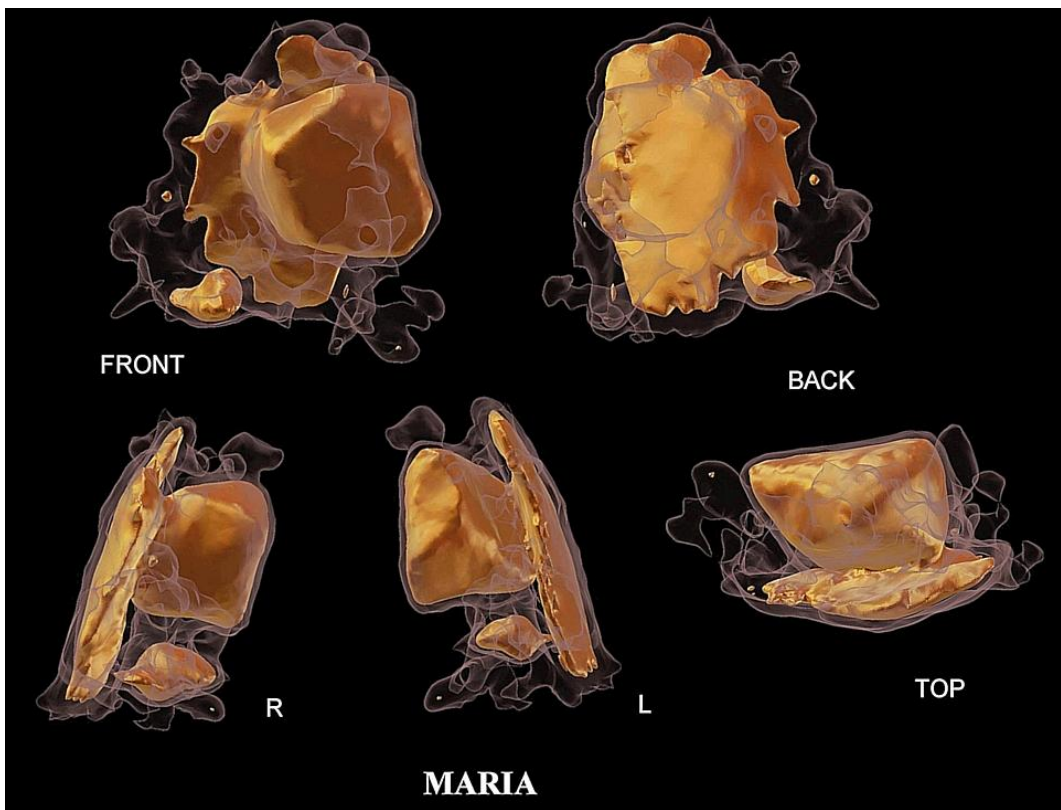


Figure 29: 3D CT showing the sacral cavity in semi-transparency and the metallic foreign bodies (*in gold*).

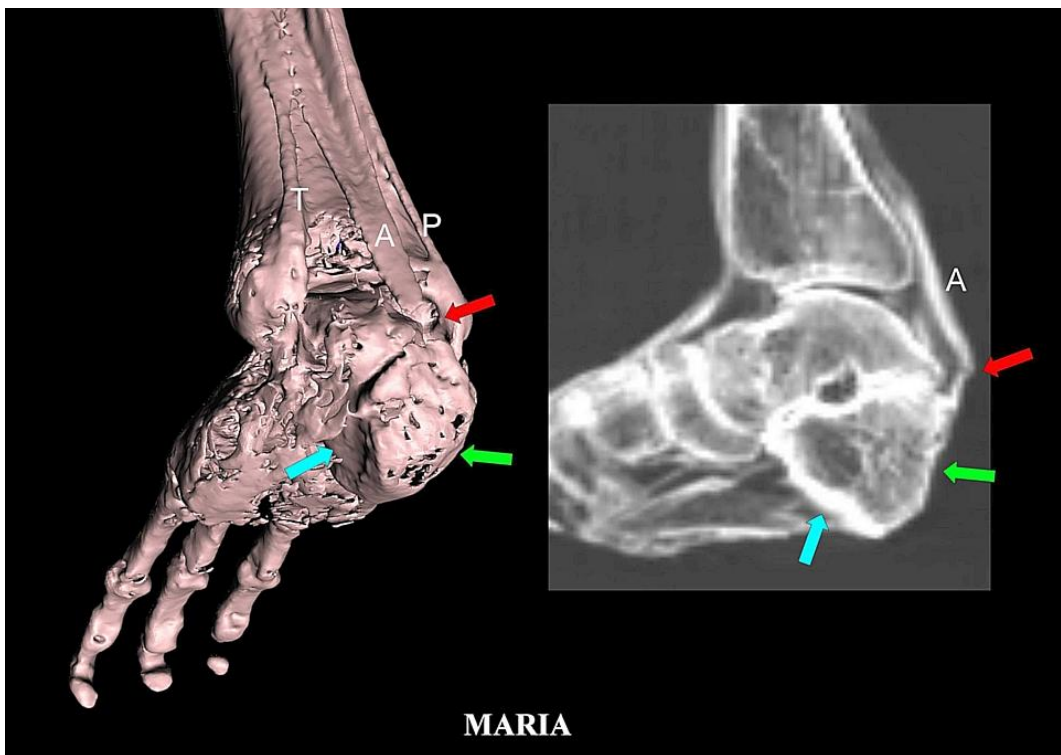


Figure 30: 3D CT (*left*) and 2D sagittal CT scan (*right*) of right heel showing truncated posterior part of the calcaneum (*green arrows*) including the attachment part of Achilles tendon (*red arrows*). Note bony regrowth at the cut end of calcaneum with thin cortex (*green arrows*) as compared with the normal thick cortex (*blue arrow*).

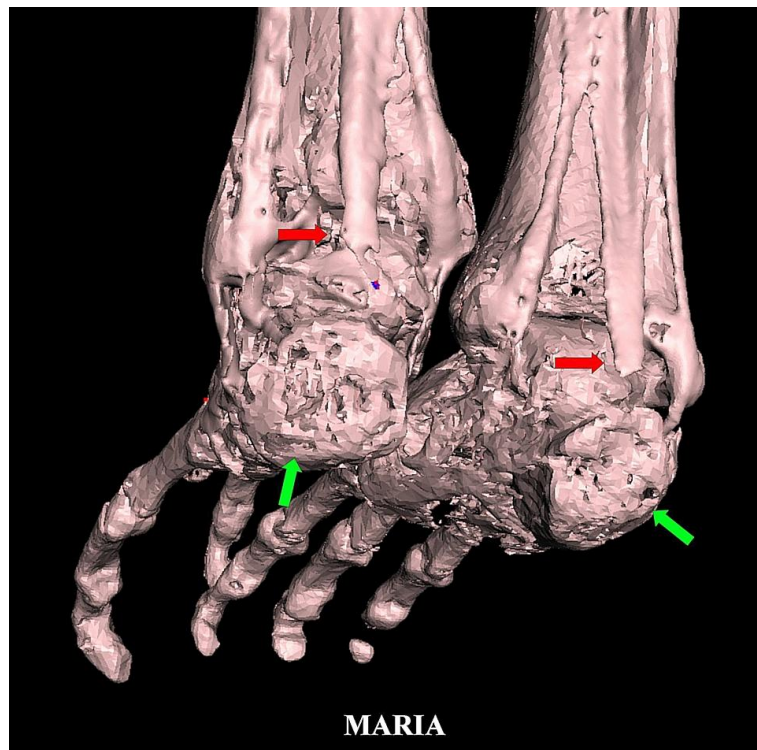


Figure 31: 3D CT showing bilateral heels. Posterior parts of both calcanei were found truncated (*green arrows*). The lower part of Achilles tendons were also cropped (*red arrows*), more in left heel.

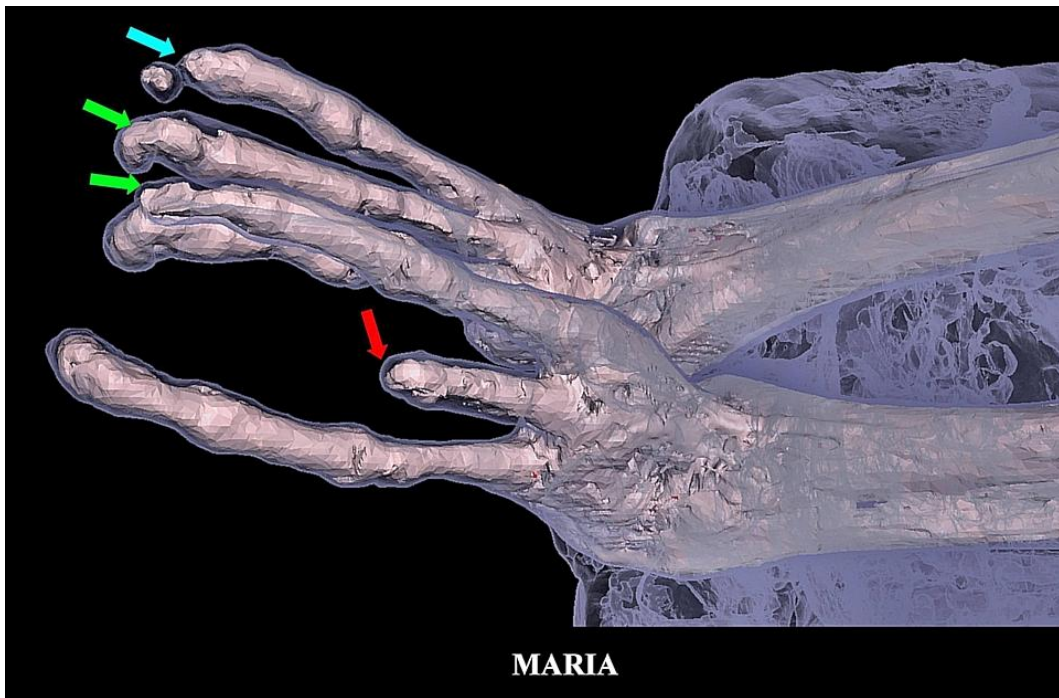


Figure 32: 3D CT showing bones through semi-transparent skin of both feet. In left foot, amputation (*red arrow*) distal to first segment (S1) was noted in middle digit. The dorsal part of the most distal segment (S4) of medial digit appeared to have been shaved off and flattened (*green arrow*). In right foot, the S3 and S4 segments of middle digit had their dorsal surface partially shaved off (*green arrow*). There was a skin constriction at the site of partial amputation of S3 and S4 segments in lateral digit. (*blue arrow*)

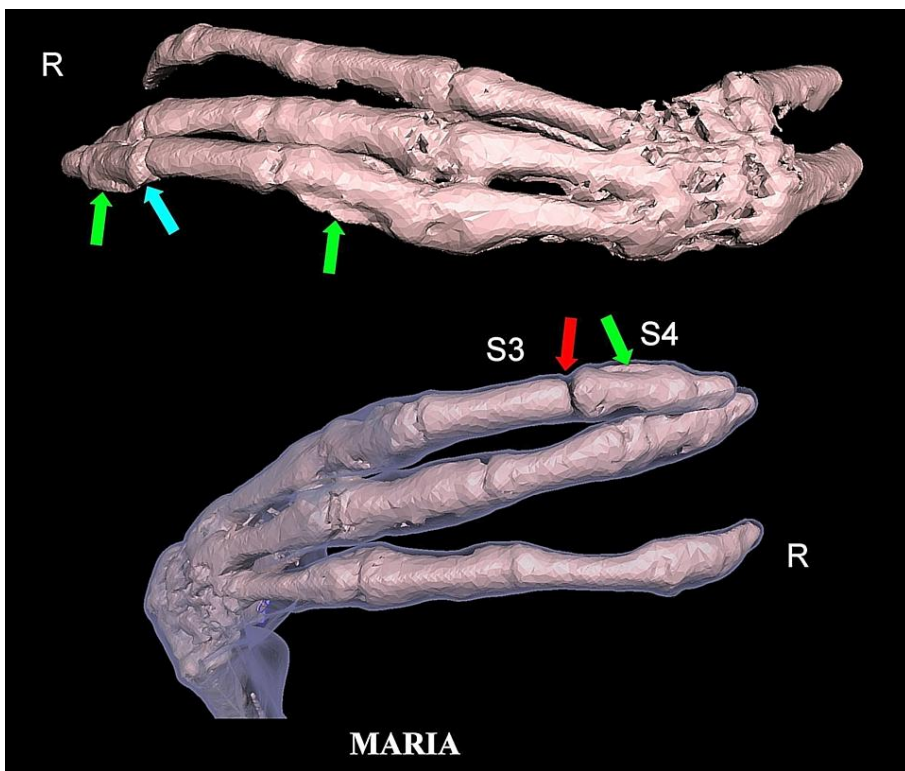


Figure 33: 3D CT showing bones in right hand (*upper*) with skin in semi-transparency (*lower*). Note the amputation in the most distal part of S3 segment of medial digit (*red arrow*) and the partial subluxation of segments S3/4 interphalangeal joint (*blue arrow*). Asymmetric subperiosteal bony thickenings (*green arrow*) were present in S2 and S4 segments of the medial digit.

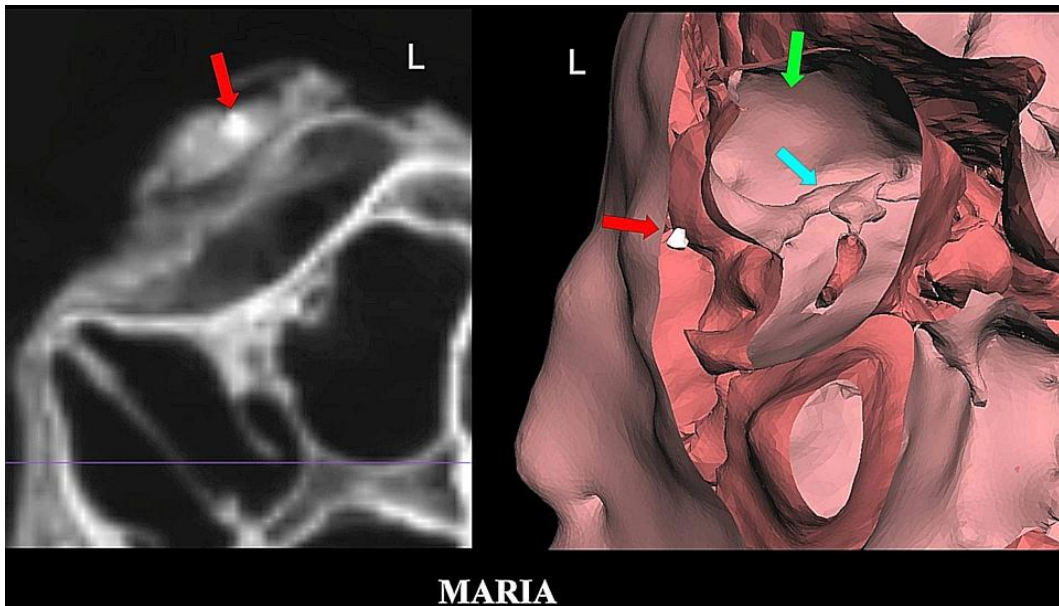


Figure 34: 2D coronal CT scan (*left*) and sagittal cut section of 3D CT (*right*) showing presence of calcification or metallic foreign body (*red arrow*) in left upper eyelid. The hyaloid canal (*blue arrow*) inside the large sized partially collapsed left eyeball can also be identified (*green arrow*).

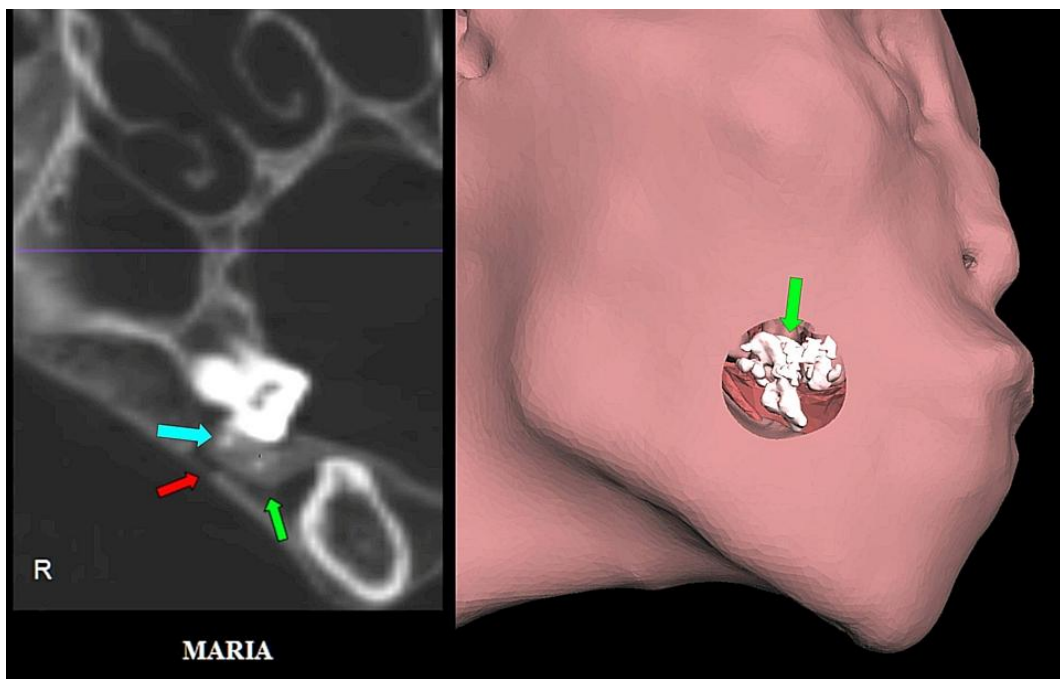


Figure 35: 2D coronal CT scan (*left*) and 3D CT of right side of face (*right*) with digital window created exposing irregular mineral content (*green arrow*) containing multi-focal tiny calcifications (*blue arrow*) deep within the right buccal wall adjacent to the R upper first and second molar teeth. A tiny skin puncture hole (*red arrow*) could be identified overlying the lesion on 2D scan.

SECTION V: COMPARATIVE ANATOMY

(A) Comparison of endocasts:

- Side by side comparison of 3D digital endocasts (*Figure 36*) of tridactyl mummies 'Maria' and 'Montserrat' and modern human was made in various projections.
- Direct volume measurement on the endocasts showed cranial volumes of 1,195,356 mm³, 1,193,459 mm³ and 1,448,922 mm³ for Maria, Montserrat and human respectively. In other words, the cranial volumes of Maria and Montserrat were similar despite difference in shape (Montserrat being more elongated in an oblique axis antero-posteriorly). The two tridactyls had cranial capacity about 17% smaller than human.
- Due to sloping frontal skull bone and smaller anterior cranial fossa, relatively small frontal lobes could be inferred.
- The cerebellum of 'Montserrat' appeared smaller.
- The convolution brain markings were most prominent on human and least prominent in 'Maria'
- Impressions due to venous sinuses were similar.

(B) Simulation of 3 fingered human hand:

- Using actual 3D CT of modern human hand, the thumb and little finger were digitally removed. Comparison of this simulated 3 fingered hand was made with the tridactyl hand of 'Maria'. (*Figure 37*) (Note: In real life, it appeared more practical to amputate near the base of the digit rather than disarticulating the whole phalange due to complex interconnected tendon and fascial attachments in hand and fingers.)
- Much longer fingers, each with 5 segments, were noted in 'Maria'. In human 4 segments were noted if the metacarpal was counted together. 'Maria' showed intact flexor and extensor tendons in digits. It appeared impossible to add an extra digit segment due to complex ligament and tendon attachments.
- In human, the segments of the fingers show progressive decrease in size distally. In 'Maria' this relationship was not observed. The 4th segments were relatively larger.
- In human, the articulated carpal bones of the removed fingers (namely, trapezium and hamate) will be jutting out from the contour of the wrist on radial and ulna sides, contrasting with conformal carpal bones of 'Maria'.
- The carpal bones of 'Maria' were more compact and smaller.

SECTION V: COMPARATIVE ANATOMY (continued)

(C) Comparison of heels:

- The heel of 'Maria' appeared relatively short. A comparison of this part of anatomy was made between tridactyl mummies 'Maria' and 'Montserrat'. (*Figures 38,39*)
- In 'Maria' 2D CT and 3D CT showed evidence of partial amputation in the posterior parts of bilateral calcanei including the insertion segments of the Achilles tendons. There was evidence of bony regrowth showing much thinner cortex.
- In 'Montserrat' with intact bone, the posterior part of calcaneum show smooth rounded outline and thick cortex. The Achilles tendon could be traced to attached to the calcaneal tuberosity via bony spur.
- Given the detachment of Achilles tendon and the shorter heels for weight bearing, mobility of 'Maria' would be severely limited. Could this be the cause for broken teeth when 'Maria' utilized her mouth to stabilize movement remained speculative.

(D) Comparison of tridactyl feet:

- Comparison of tridactyl feet of 'Maria', 'Montserrat' was made with modern human foot. (*Figures 40,41,42*).
- The tridactyl feet were smaller than that of human.
- 'Maria' appeared more skinny as compared with 'Montserrat' due to aging change or disuse atrophy.
- High plantar arch was noted in 'Montserrat', flat foot was noted in 'Maria'.
- Weight bearing soft tissue pads were noted in medial digits of all, consistent with similar biomechanics in bipedal posture.
- Wide gap was found between all digits in tridactyls. Only the big toe showed wide separation with the second toe in human. Very tight spaces were found between other toes in human.
- The proportion of bone segments in digits of tridactyls was quite different from human.

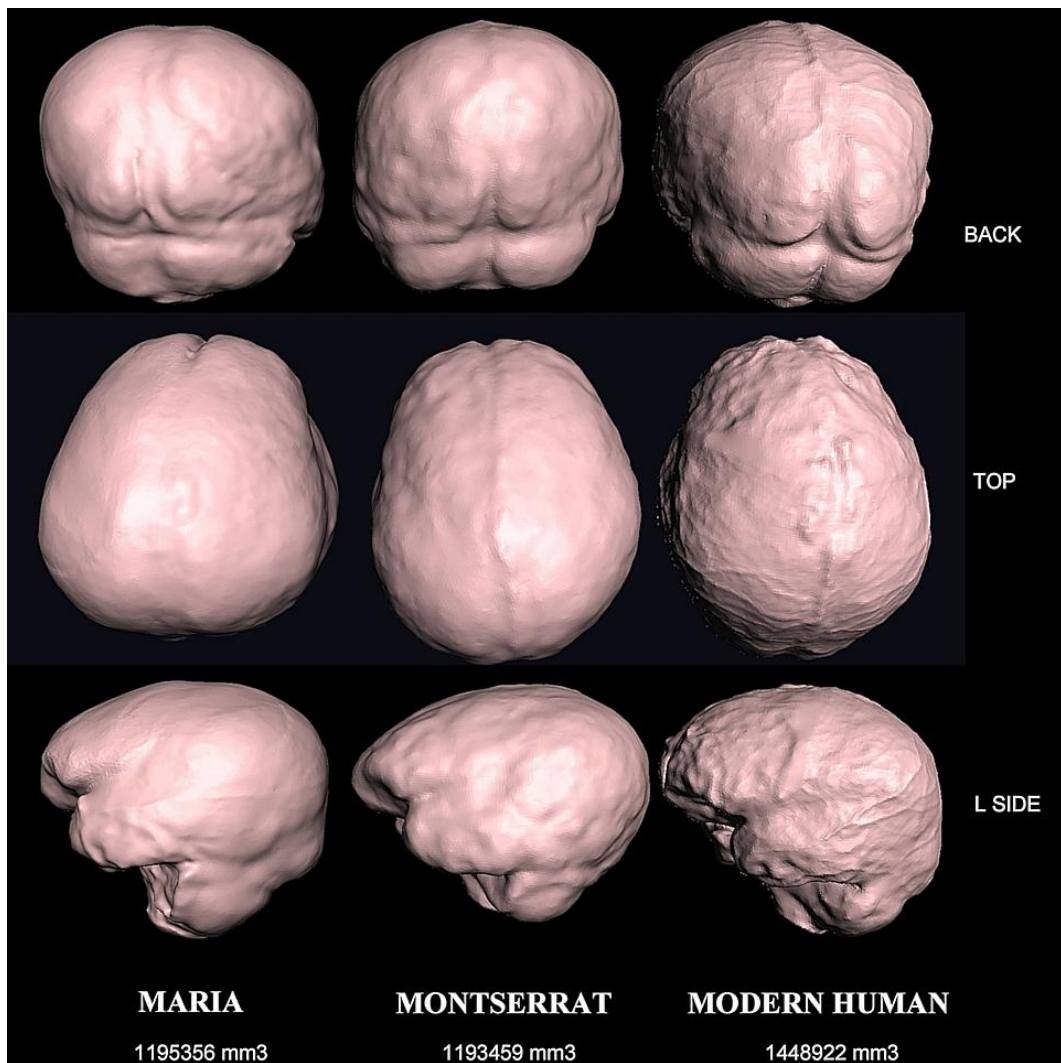


Figure 36: Comparison of 3D virtual cranial endocasts created from CT datasets of Maria (*left*), Montserrat (*middle*) and modern human (*right*). Note the direct volume measurement from the 3D models showed the cranial capacity of Maria and Montserrat were similar and smaller than normal human.

The region representing frontal lobes were small in both Maria and Montserrat. Cerebellum seemed to be smallest in Montserrat and largest in Maria. Convolution markings were most pronounced in human and least so in Maria.

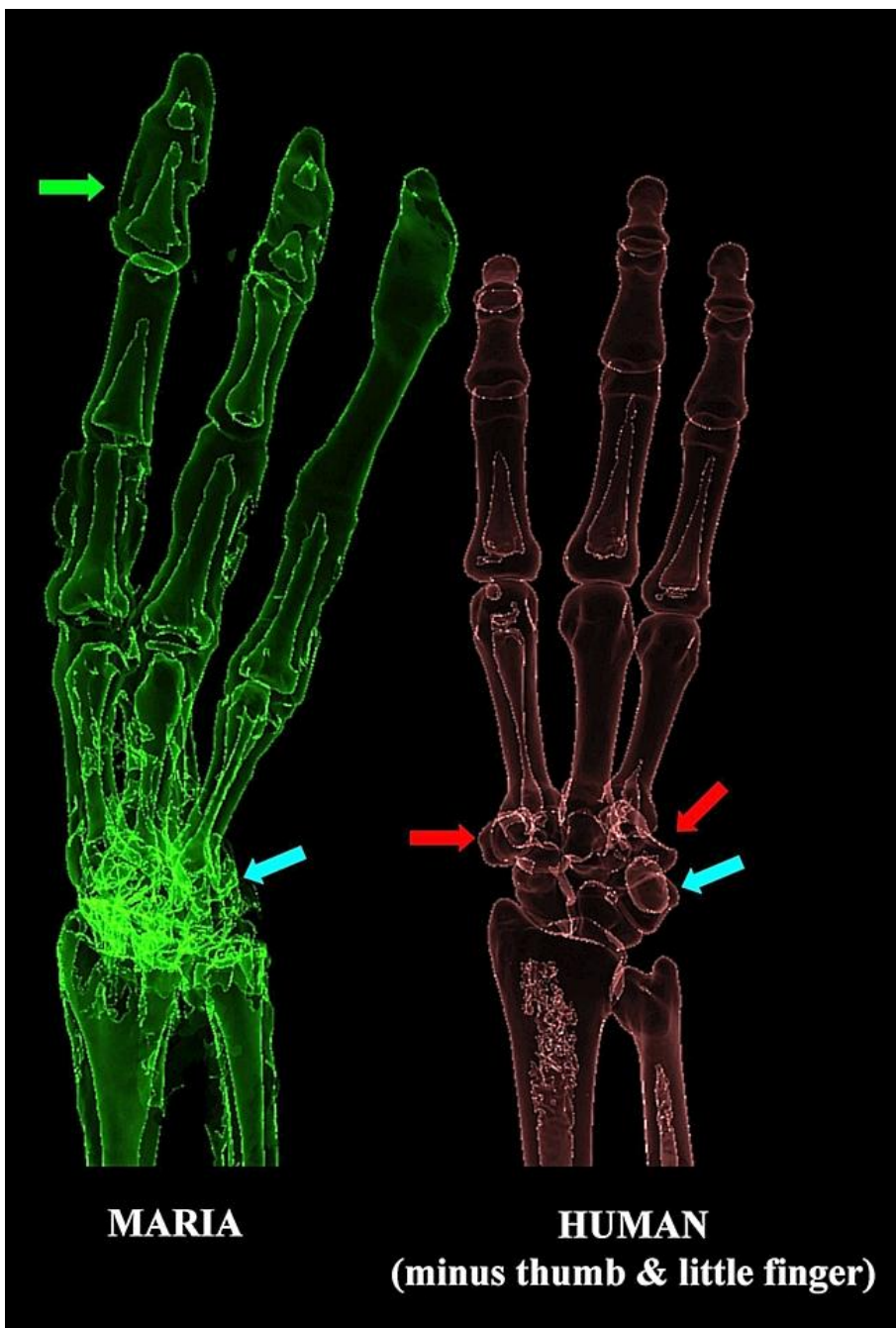


Figure 37: Comparison of 3D CT in semi-transparency of right hand of Maria (*left*) and modern human (*right*) with software removal of thumb and little finger to simulate 3-fingered hand for comparison purpose. Note the projecting carpal bones (*red arrows*) namely trapezium and hamate in human. Pisiform (*blue arrows*) in Maria appeared much smaller relative to human. In human, the digits show progressively smaller size distally but in Maria, S4 segment (*green arrow*) appeared particularly prominent.

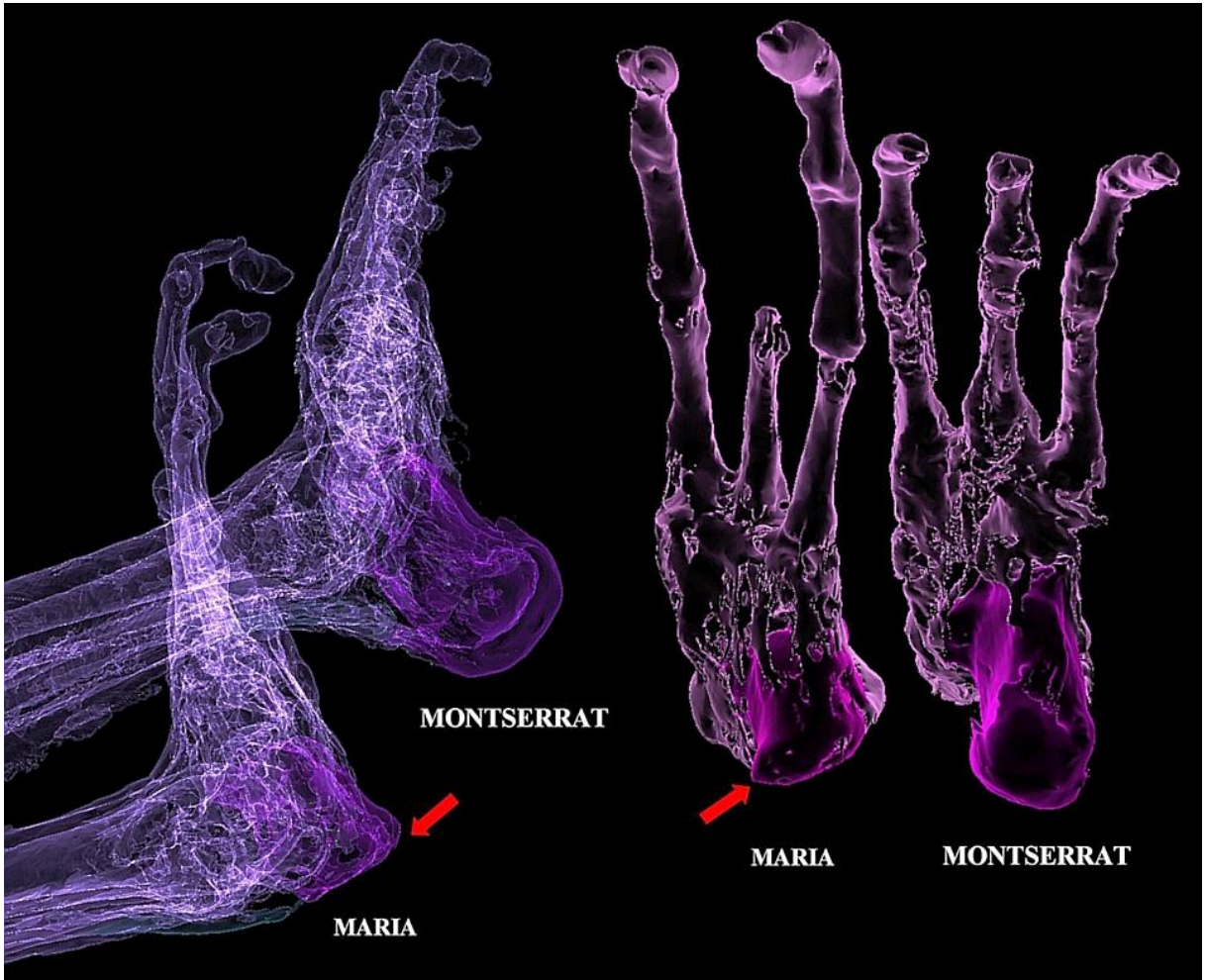


Figure 38: Comparison of 3D CT in semi-transparency between the heels of Maria and Montserrat. Noted the truncated posterior part of the calcaneum of Maria showed very thin bony cortex (*red arrow*) with sharp margin relative to the rest of calcaneum contrasting with the relatively thick cortex and rounded appearance in Montserrat.

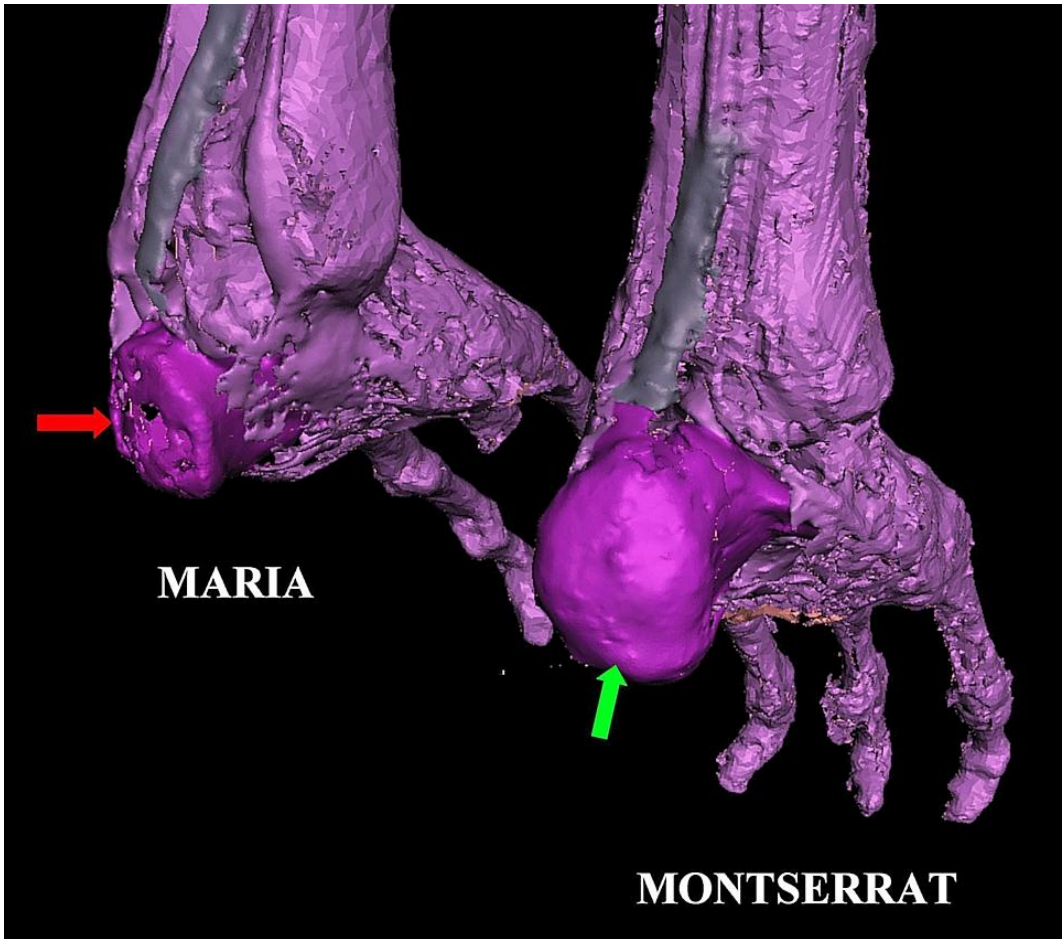


Figure 39: Comparison of 3D CT of Maria (*left*) and Montserrat (*right*) showing the truncated appearance in posterior part of the calcaneum (*red arrow*) in Maria contrasting with the rounded intact calcaneum (*green arrow*) in Montserrat. Also note the truncated Achilles tendon in Maria. The intact Achilles tendon in Montserrat can be traced to the calcaneal tuberosity.

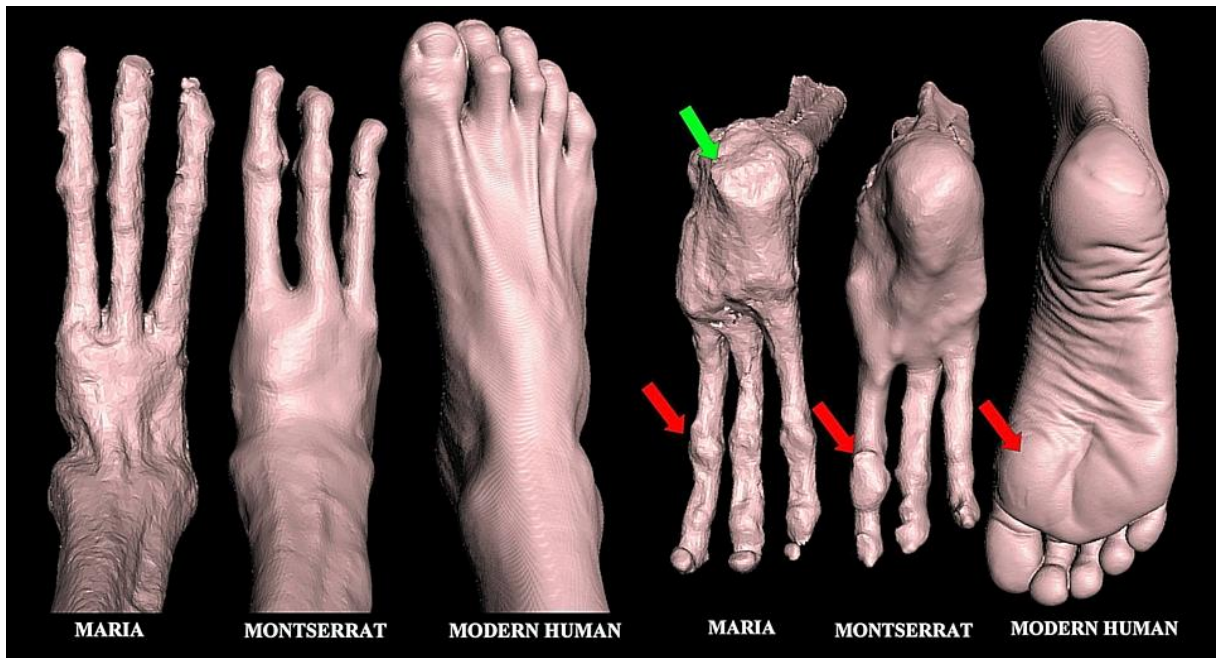


Figure 40: Comparison of 3D CT of right foot of Maria, Montserrat and modern human. Note the soft tissue pad over medial digits (*red arrows*) suggestive of weight-bearing points in addition to heel pads. Soft tissue in Maria appeared more atrophic than Montserrat. The heel of Maria appeared truncated and shortened (*green arrow*).

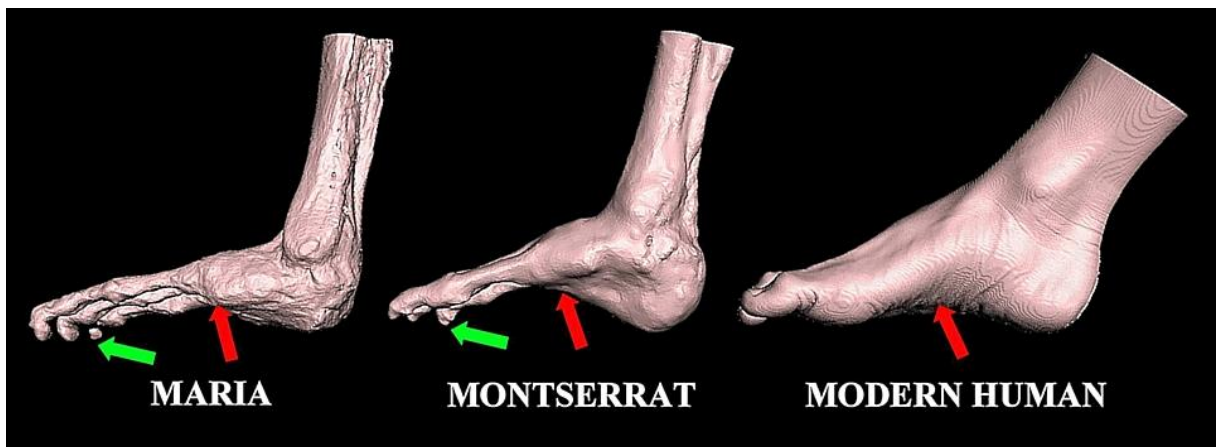


Figure 41: Comparison of 3D CT of right foot of Maria (*left*), Montserrat (*middle*) and modern human (*right*). Note the difference in plantar arches (*red arrows*) and the length of digits. Claw-like deformities in the most distal segments of digits (*green arrows*) in Maria and Montserrat were noted, more pronounced in Maria.

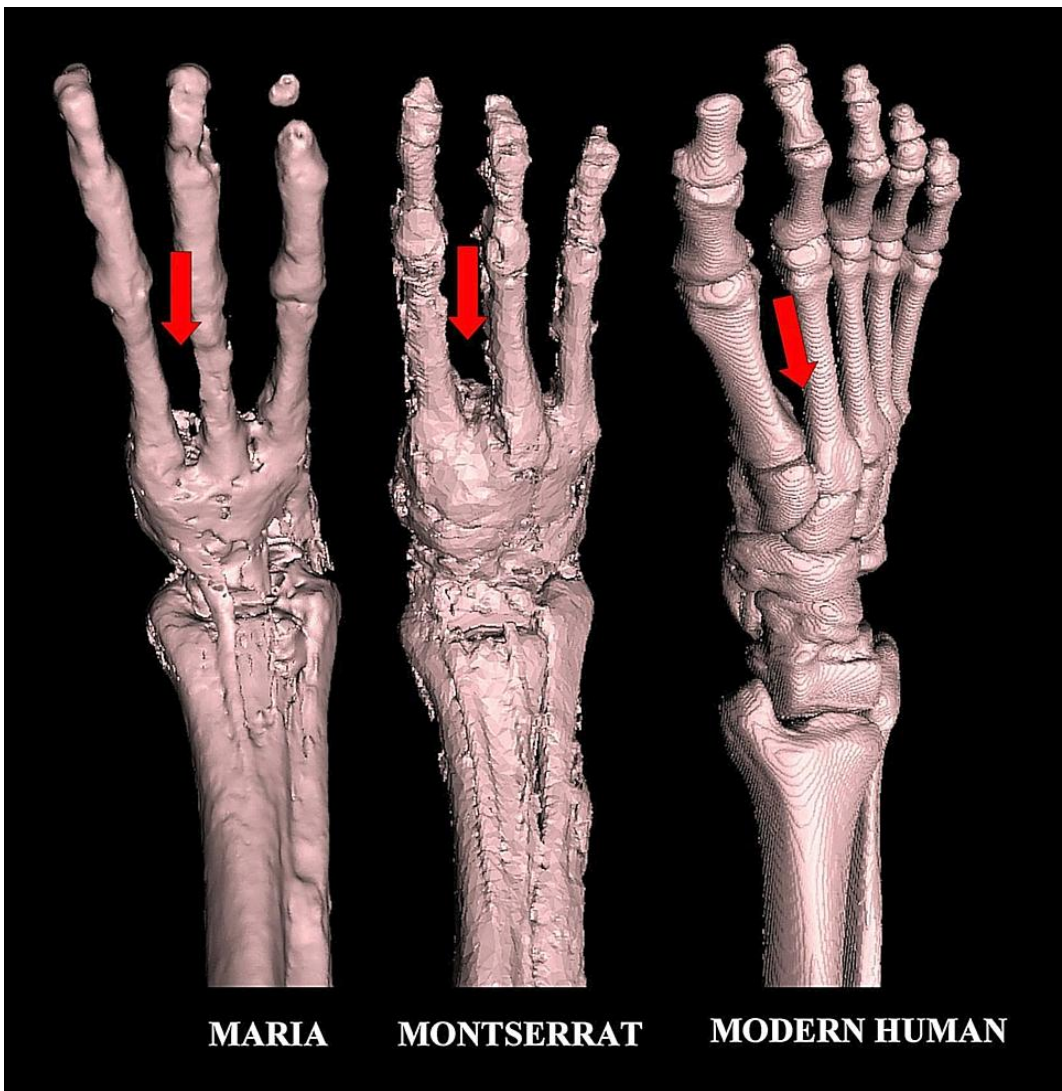


Figure 42: Comparison of 3D CT showing bones of right foot of Maria (*left*), Montserrat (*middle*) and modern human (*right*). Note the wide gap (*red arrows*) between all digits in Maria and Montserrat but only in big toe in modern human. The bones in digits also showed difference in length, diameter and shape. The tarsal bones appeared more compact in Maria and Montserrat than human.

SECTION VI: CONCLUSION

- Due to its good preservation status and intact internal anatomy, the tridactyl mummy 'Maria' provided a good source of knowledge into significant variations in anatomy so far unknown to modern human. It had helped to project our knowledge into the past world.
- The evidence confirmed 'Maria' to be a tridactyl bipedal hominid with basic human construction but showing significant anatomical differences, including tridactyls and anomalous craniofacial features.
- 'Maria' appeared to possess an aged skeleton relative to tridactyl mummy 'Montserrat'.
- 'Maria' was found to be suffering from severe illness i.e. disseminated cancer affecting the spine and hips resulting in spinal alignment problem. Could the absence of left breast be evidence of mastectomy for breast carcinoma?
- 'Maria' also suffered from multiple trauma including large area of bone and tissue loss in lower pelvic area and perineum. This major trauma could have been devastating and fatal injury. Puncture wounds were present ? due to animal bite marks.
- The left pelvic bone might be harbouring a suspicious metallic implant of unusual shape and uncertain origin.
- Mutilations in toes could have been due to post-mortem changes but signs of old trauma in calcanei and medial digit in right hand remained suspicious of pre-mortem insult.
- If the suspected cataract 'lens' in 'Maria' could be retrieved and confirmed, it would have been a significant archaeological find providing insight into the visual system of these large eyeball individuals.
- Given the finding of Y chromosome in DNA analysis of 'Maria' and the presence of female phenotype including presence of well formed right breast, possibility of Swyer Syndrome has to be considered.

SECTION VII: CAUSE OF DEATH

'Maria' suffered from late stage cancer with bony metastases but the immediate cause of death would likely be due to major trauma with fracture sacrum and extensive tissue loss in lower posterior pelvic area and perineum causing disruption of the pelvic floor.

ABOUT DR. FUNG

Dr. K H Fung is a retired radiologist with over 40 years of experience in diagnostic radiology. His special interests include 3D medical visualization, interventional radiology and neuro-intervention.

Dr. Fung is also an artist in the domain of intersection of art and science utilising his expertise in 3D medical visualization. Dr. Fung was the first place co-winner in the '2007 International Science & Engineering Visualization Challenge' organized by Science magazine and National Science Foundation (USA).

His artworks had been exhibited in museums in various countries including USA, Europe, China, Australia and Hong Kong.

He had current exhibits in 2025 in the Hong Kong Museum of Medical Sciences (featuring stereoscopic 3D and 4D medical imaging and art) and in Nina Park (featuring the Nina wood fossils collection) in Hong Kong.

Through his collaboration with Science Photo Library, his interdisciplinary artworks bridging art and science had been made available to various international renowned digital media, magazines, books, and journals.

/end